Cosmological Reionization and the End of the Dark Ages

Paul R. Shapiro

University of Texas at Austin

Texas Cosmology Network Meeting

University of Texas at Austin

September 15, 2006

The Epoch of Reionization

- Absorption spectra of quasars have long shown that the intergalactic medium at redshifts $z < 6$ is highly ionized, with a residual neutral H atom concentration of less than 1 atom in 10^4 .

  ===> universe experienced an “epoch of reionization” before this.

The Epoch of Reionization

- Absorption spectra of quasars have long shown that the intergalactic medium at redshifts $z < 6$ is highly ionized, with a residual neutral H atom concentration of less than 1 atom in 10^4 .

  ===> universe experienced an “epoch of reionization” before this.
- Sloan Digital Sky Survey quasars have been observed at $z > 6$ whose absorption spectra show dramatic increase in the H I fraction at this epoch as we look back in time ===>

  ===> epoch of reionization only just ended at $z \gtrsim 6$.

The Epoch of Reionization

- Absorption spectra of quasars have long shown that the intergalactic medium at redshifts $z < 6$ is highly ionized, with a residual neutral H atom concentration of less than 1 atom in 10^4 .

  ===> universe experienced an "epoch of reionization" before this.
- Sloan Digital Sky Survey quasars have been observed at $z > 6$ whose absorption spectra show dramatic increase in the H I fraction at this epoch as we look back in time.

  ===> epoch of reionization only just ended at $z \gtrsim 6$.
- The cosmic microwave background (CMB) exhibits polarization which fluctuates on large angular scales; WMAP finds that almost 10% of the CMB photons were scattered by free electrons in the IGM

  ===> IGM must have been ionized much earlier than $z = 6$ to supply enough electron scattering optical depth

  ===> reionization already substantial by $z \gtrsim 11$

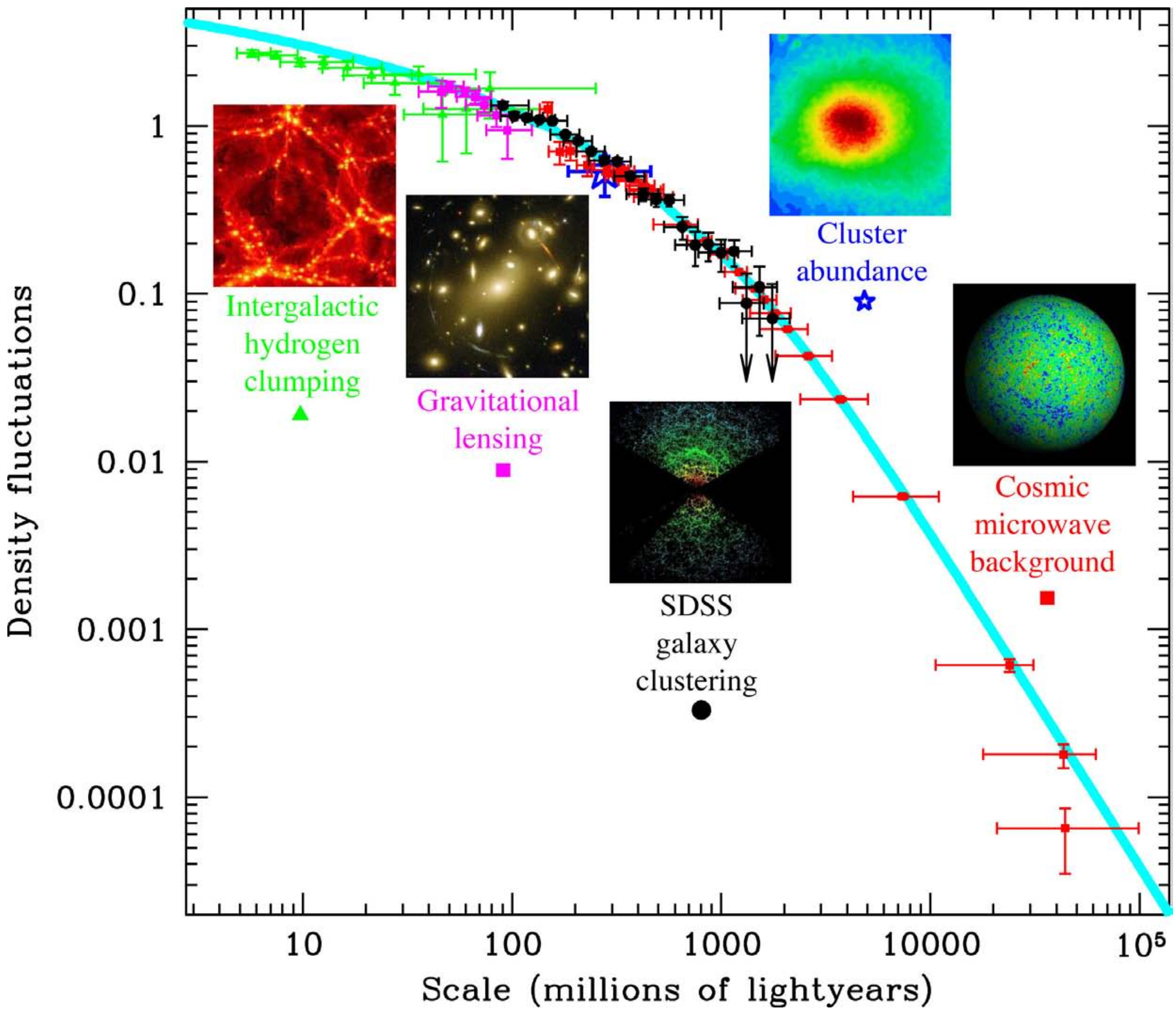

Density fluctuations
1
0.1
0.01
0.001
0.0001
10
100
1000
10000
10^5
Scale (millions of lightyears)
Intergalactic hydrogen clumping
Gravitational lensing
SDSS galaxy clustering
Cluster abundance
Cosmic microwave background

WMAP 1yr vs 3yr

- Lower amplitude and increased tilt of power spectrum
  → fewer halos form on small scales at given redshift
  → sources of reionization much rarer at same epochs

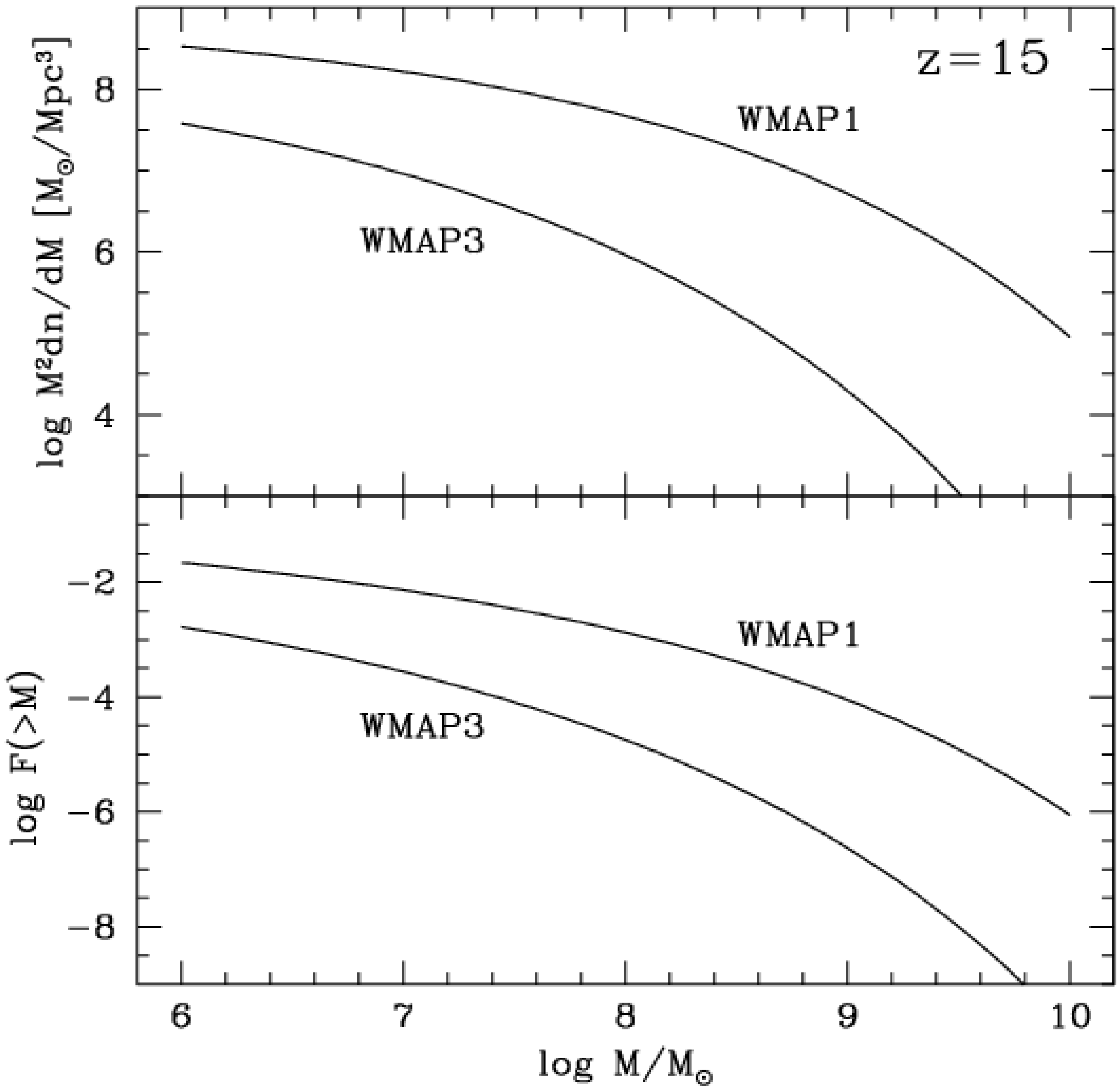

Structure formation in ΛCDM at z = 10

simulation volume = $(100\ h^{-1}\mathrm{Mpc})^3$, comoving

1624^3 particles on 3248^3 cells

Projection of cloud-in-cell densities of 20 Mpc slice

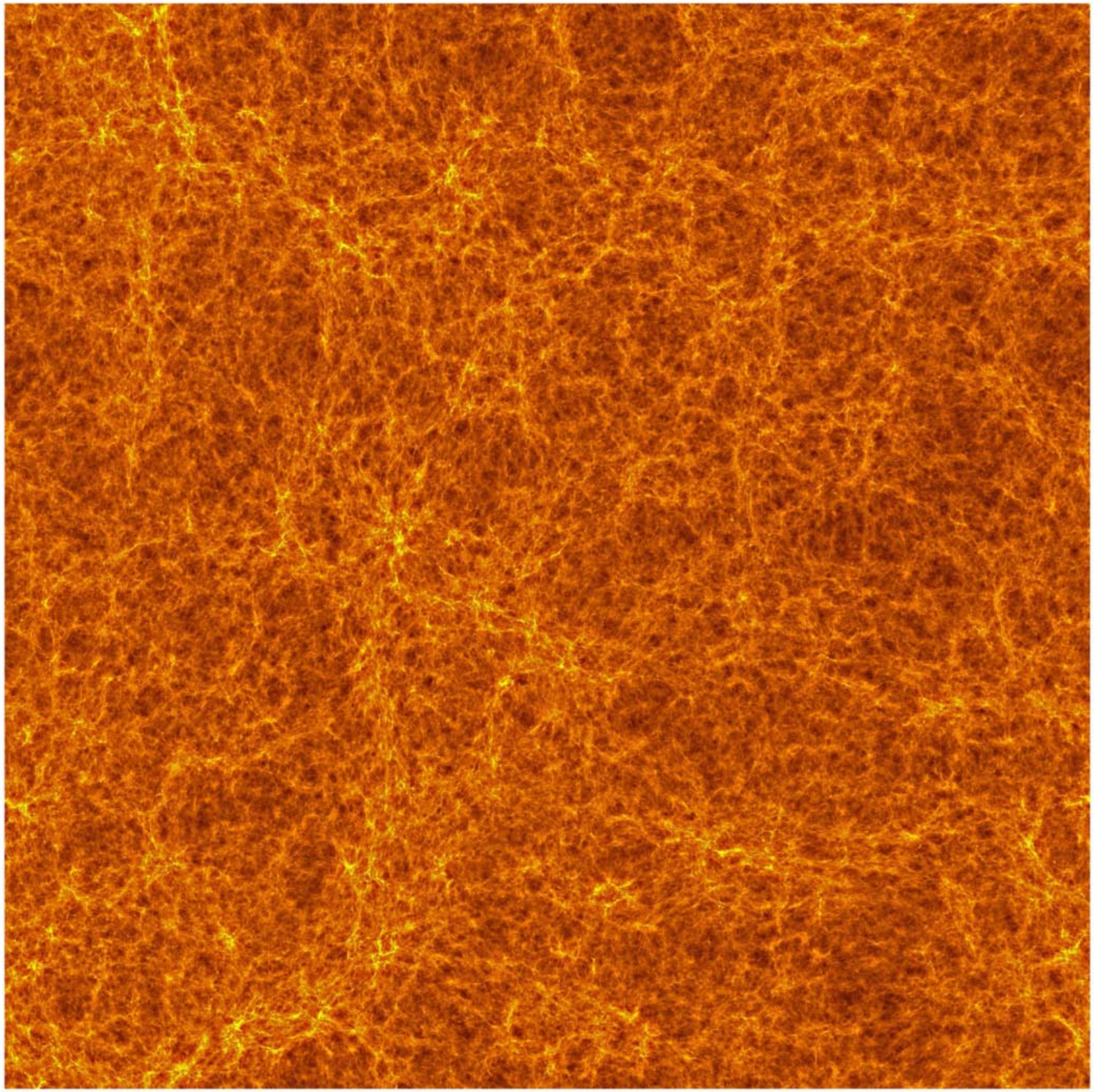

A Dwarf Galaxy Turns on at z=9

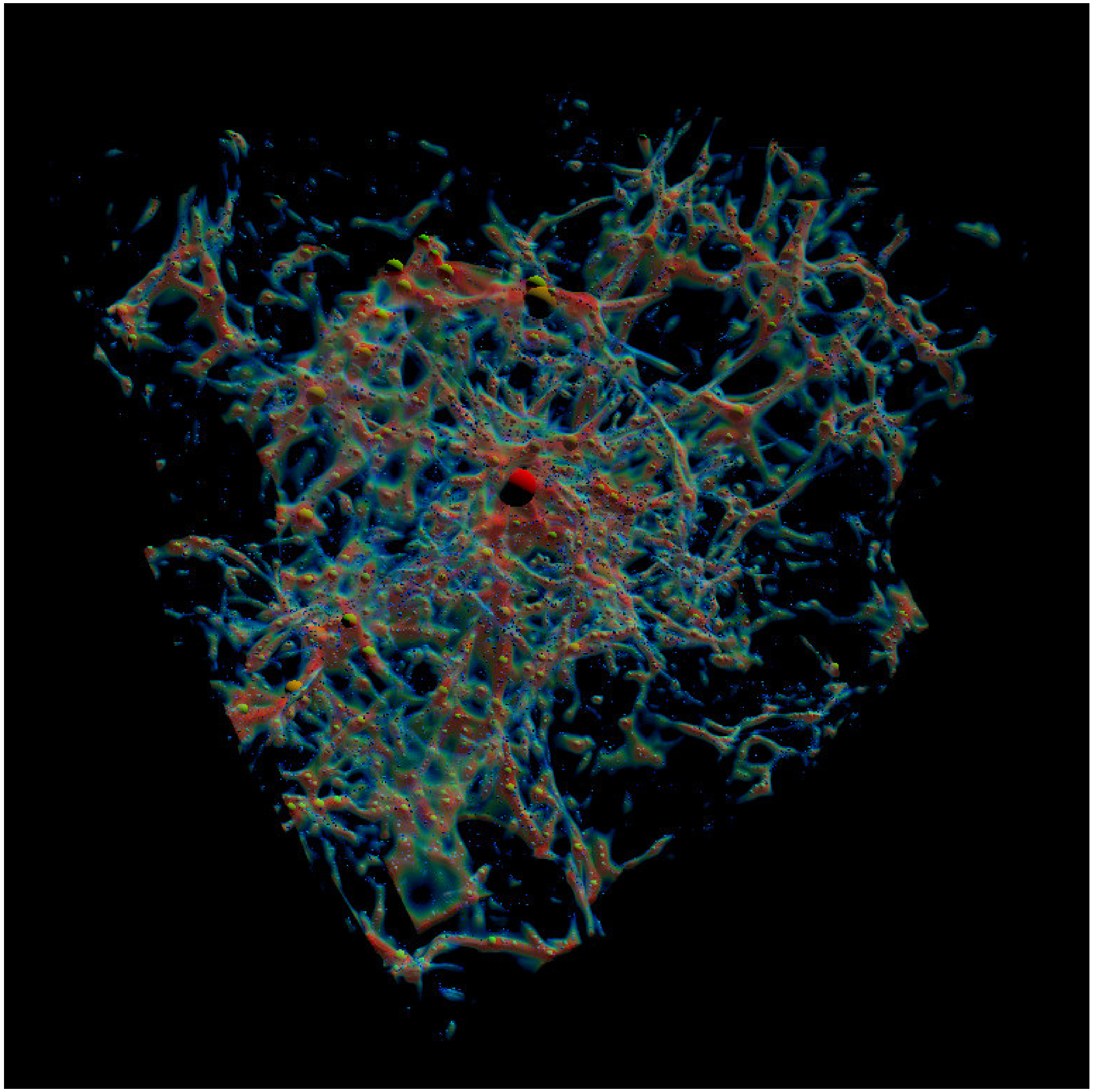

Simulating Cosmic Reionization at Large Scales I. : The Geometry of Reionization

Iliev, Mellema, Pen, Merz, Shapiro & Alvarez (2006)

MNRAS, 369, 1625 (astro-ph/0512187)

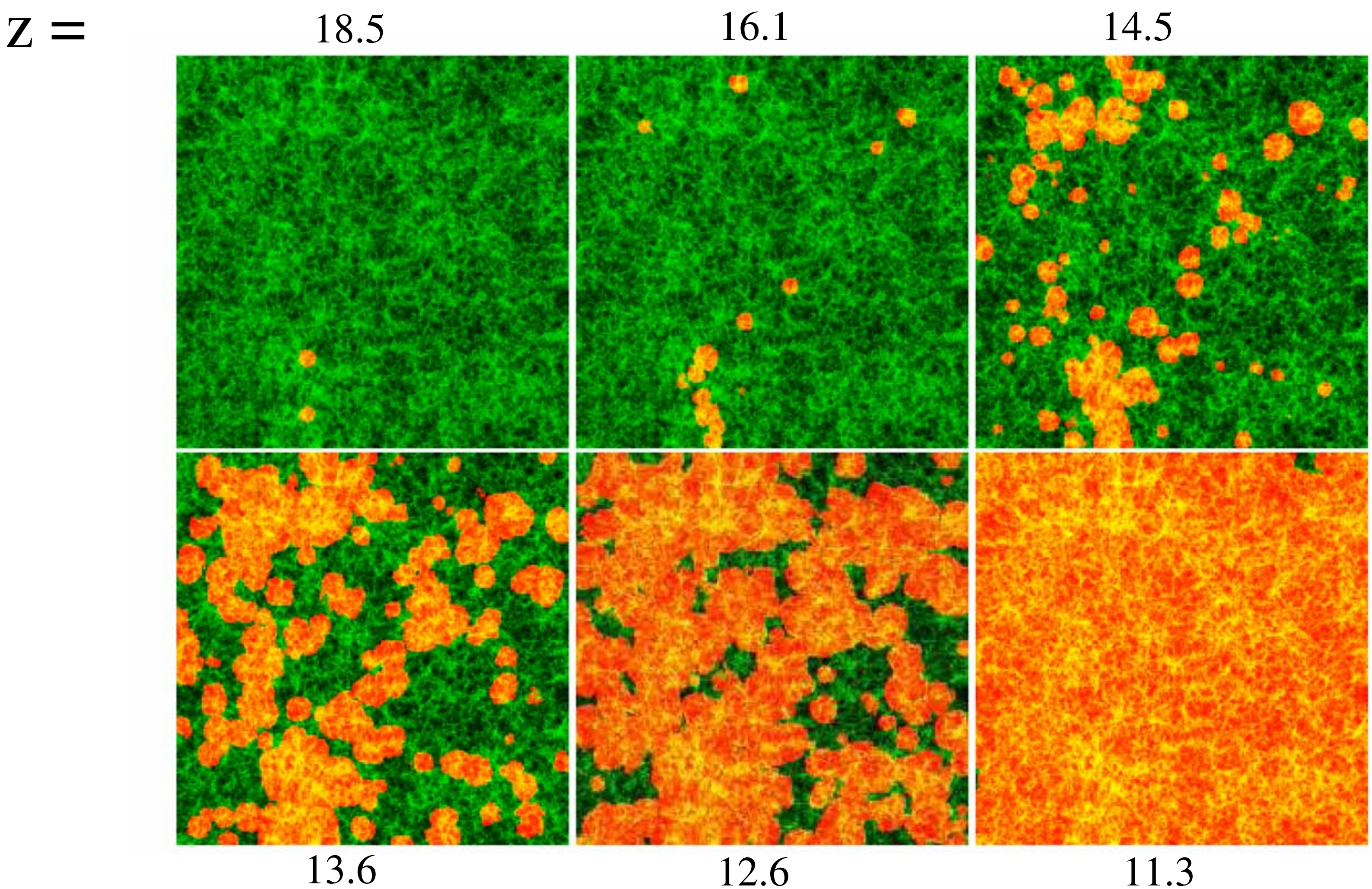

C^2 – Ray : A New Method for Photon-Conserving Transport of Ionizing Radiation

Mellema, Iliev, Alvarez & Shapiro (2006) New Astronomy, 11, 374

(astro-ph/0512187)

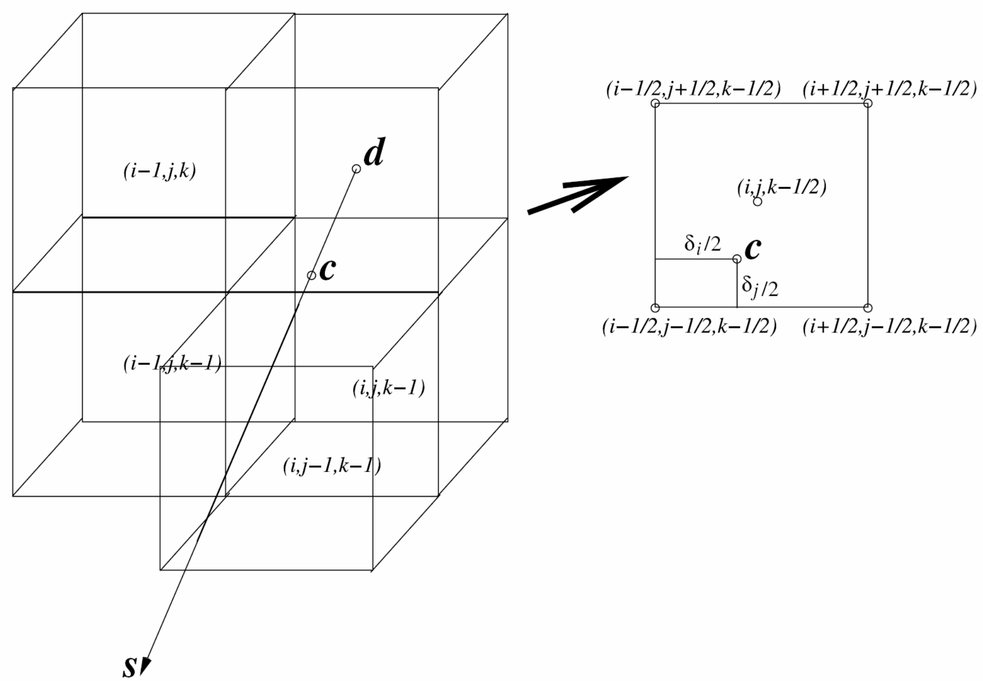

Fig. A.1. Short-characteristics ray tracing.

Dynamical H II Region Evolution in Turbulent Molecular Clouds

Mellema, Arthur, Henney, Iliev & Shapiro (2006) ApJ, 647, 397 (astro-ph/0512187)

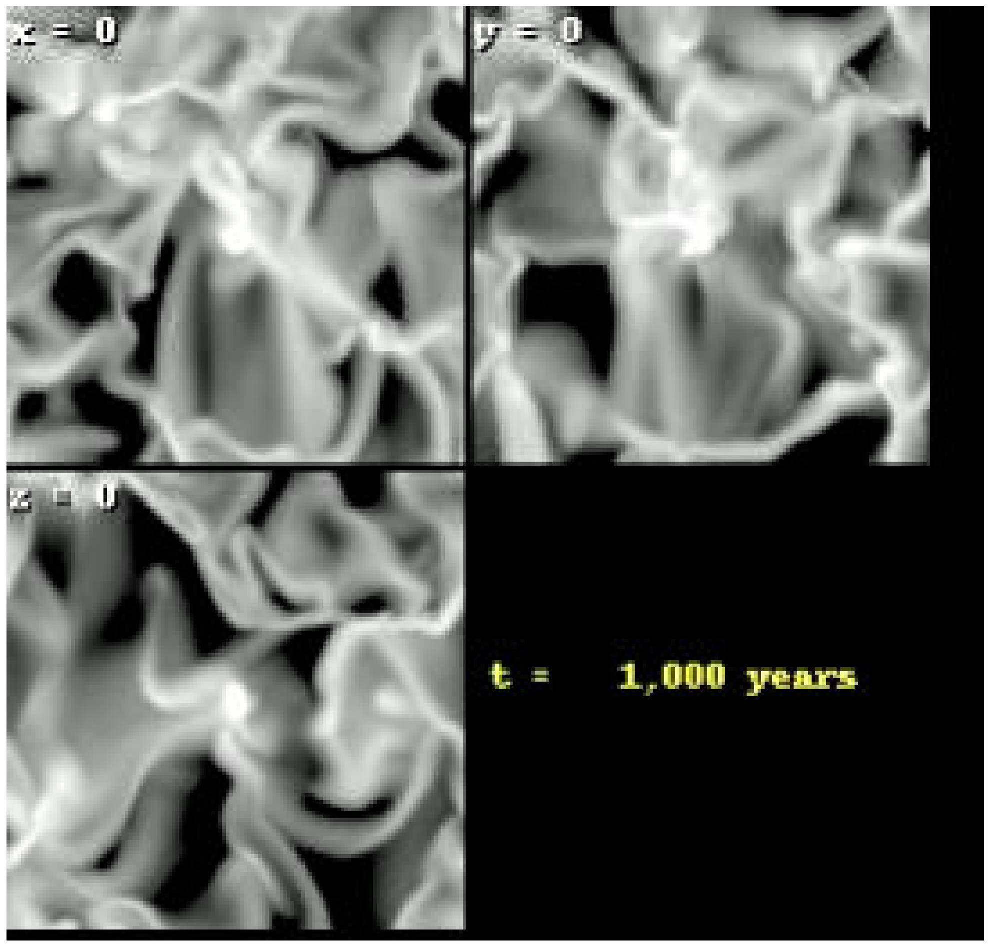

Dynamical H II Region Evolution in Turbulent Molecular Clouds

Mellema, Arthur, Henney, Iliev & Shapiro (2006) ApJ, 647, 397 (astro-ph/0512187)

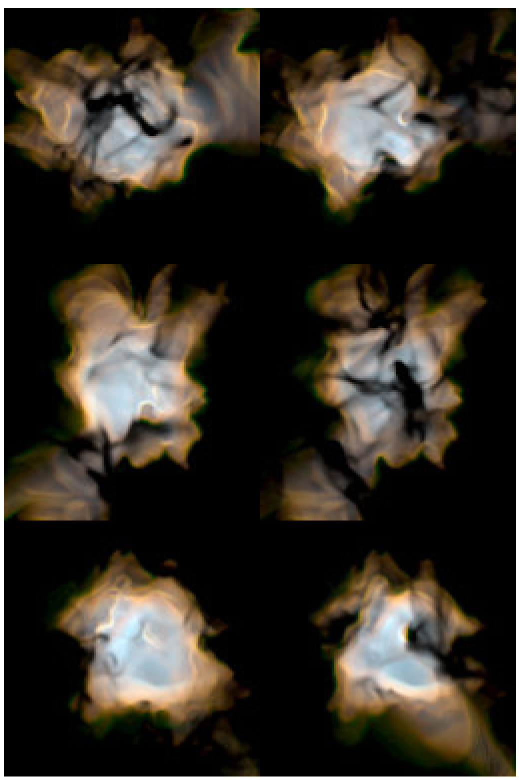

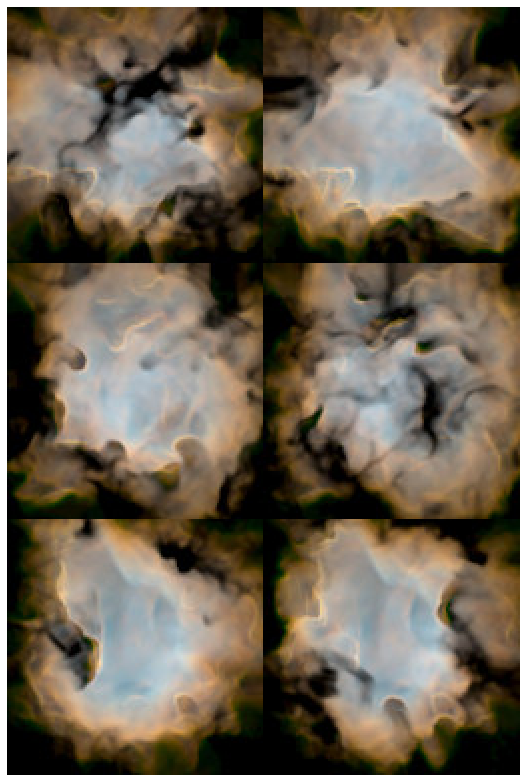

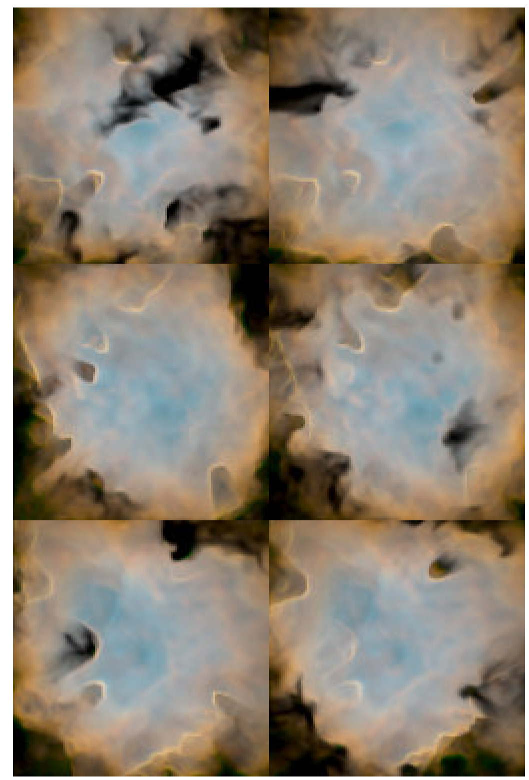

Simulating Reionization at Large Scales II : The 21-cm Emission Features and Statistical Signals

Mellema, Iliev, Pen, & Shapiro (2006), MNRAS, in press

(astro-ph/0603518)

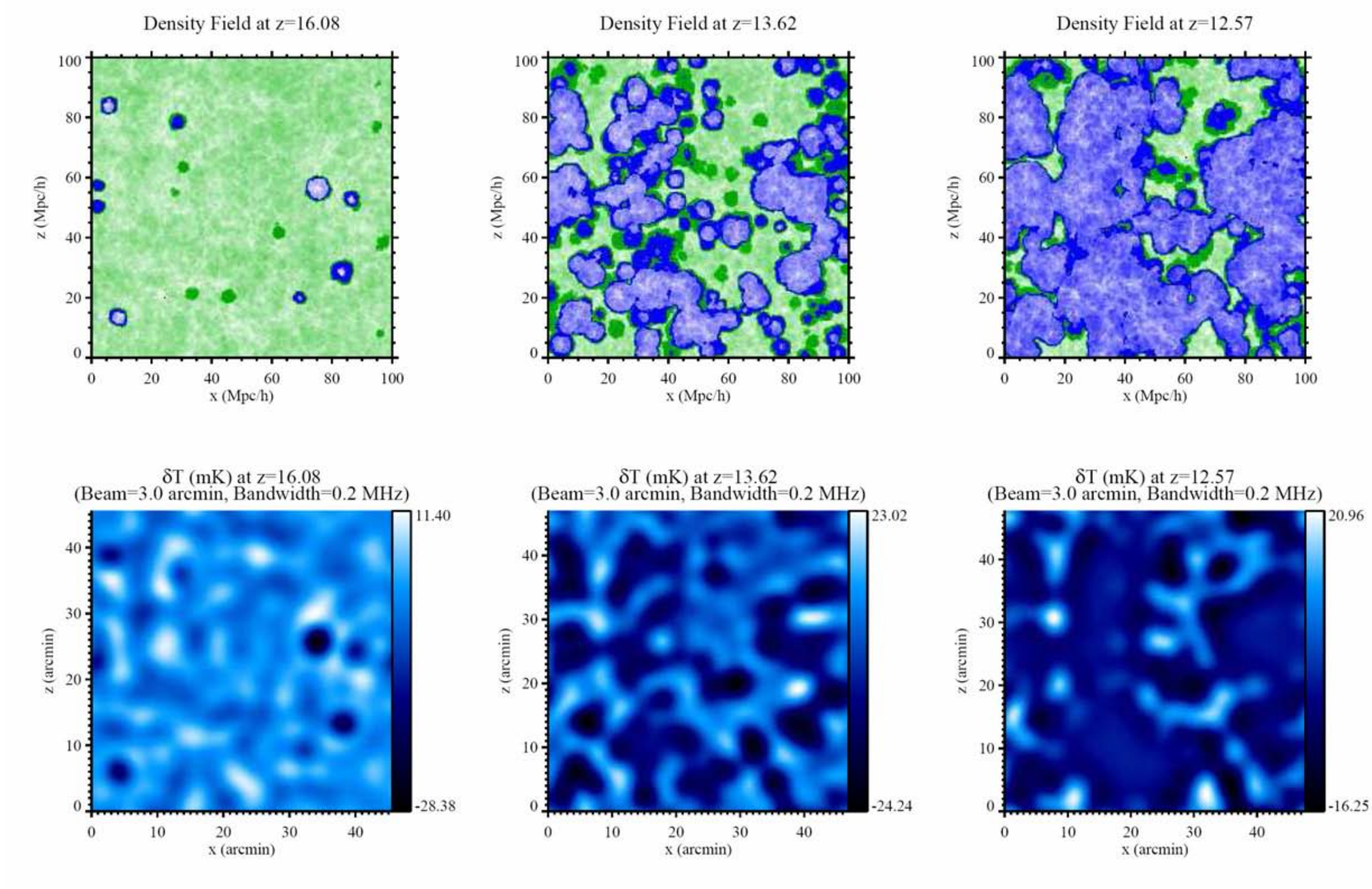

Low Frequency Array (LOFAR)

Mileura Wide-field Array (MWA)

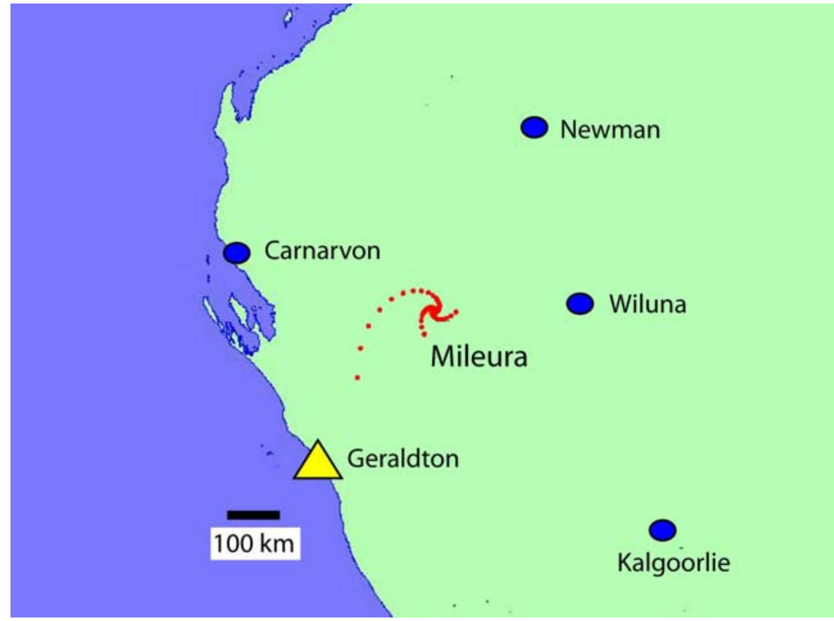

PrimevAl Structure Telescope (PAST)

Prototype Tests, Ulastai, Xin Jiang, China

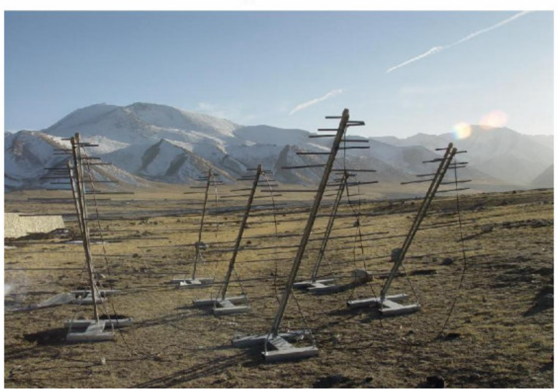

Square Kilometer Array (SKA)

Cosmological Radiative Transfer Codes Comparison Project I. : The Static Density Field Tests

Iliev, Ciardi, ..., Shapiro, ... (2006) MNRAS, 371, 1057

(astro-ph/0603518)

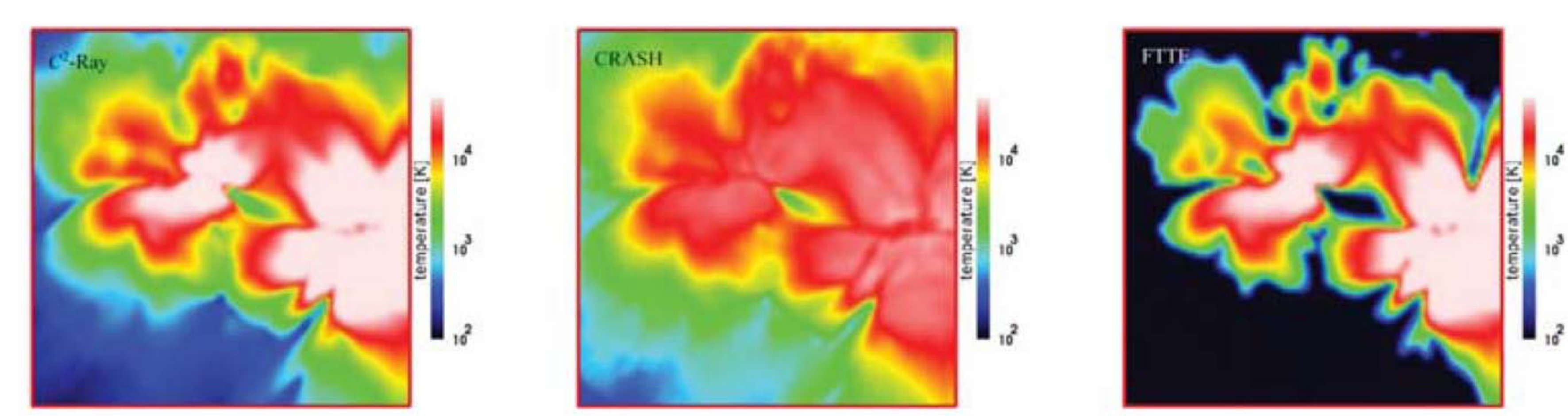

Relativistic Ionization Fronts

Shapiro, Iliev, Alvarez, & Scannapieco (2006) ApJ, in press

(astro-ph/0507677)

The H II Region of the First Star

Alvarez, Bromm, & Shapiro (2006) ApJ, 639, 621

(astro-ph/0507684)

The Effect of Minihalos on Reionization

Ciardi, Scannapieco, Stoehr, Ferrara, Iliev & Shapiro (2006), MNRAS, 366, 689

(astro-ph/0507684)

The 21-cm Background from the Cosmic Dark Ages: Minihalos and the Intergalactic Medium Before Reionization

Shapiro, Ahn, Alvarez, Iliev, Martel & Ryu (2006), ApJ, 646, 681

(astro-ph/0512516)

The Cosmic Reionization History as Revealed by the CMB Doppler – 21 cm Correlation

Alvarez, Komatsu, Dore & Shapiro (2006), ApJ, 647, 840

(astro-ph/0512010)

UV pumping of hyperfine transitions in the light elements, with application to 21-cm hydrogen and 92-cm deuterium lines from the early universe

Chuzhoy and Shapiro (2006) ApJ, in press

(astro-ph/0512206)

Heating and Cooling of the Intergalactic Medium By Resonance Photons

Chuzhoy and Shapiro (2006) ApJL, submitted

(astro-ph/0604483)

Recognizing the First Radiation Sources Through Their 21-cm Signature

Chuzhoy, Alvarez &Shapiro (2006), ApJL, 648, 1

(astro-ph/0605511)

The Kinetic Sunyaev-Zel'dovich Effect from Radiative Transfer Simulations of Patchy Reionization

Iliev, Pen, Bond, Mellema, & Shapiro (2006), ApJ, submitted; and

(2006) New Astronomy Reviews, in press

(astro-ph/0607209)

Self-Regulated Reionization

Iliev, Mellema, Shapiro, & Pen (2006), MNRAS, submitted;

(astro-ph/0607517)

Does Radiative Feedback by the First Stars Promote or Prevent Second Generation Star Formation?

Ahn & Shapiro (2006), MNRAS, submitted;

(astro-ph/0607642)

Implications of WMAP Three-Year Data For the Sources of Reionization

Alvarez, Shapiro, Ahn, and Iliev (2006), ApJL, 644, 101
(astro-ph/0604447)

Simulating Cosmic Reionization at Large Scales I. : The Geometry of Reionization

Iliev, Mellema, Pen, Merz, Shapiro & Alvarez (2006)
MNRAS, 369, 1625

(astro-ph/0512187)

- The first, truly large-scale, radiative transfer simulations of cosmic reionization, comoving volume $(143\ \mathrm{Mpc})^3$, with high enough resolution to account for individual dwarf galaxy sources.

- This is more than a 2 orders of magnitude improvement over previous simulations.

- We achieve this by combining results from extremely large, cosmological N-body simulations with our new, fast and efficient code for 3D radiative transfer, **C^2-Ray**.

N-body + Radiative Transfer ➔ Reionization simulation

- N-body simulation yields the density field and sources of ionizing radiation
  - PMFAST code (Merz, et al. 2005) with 1624^3 = 4.28 billion particles, 3248^3 cells, particle mass = 2.5×10^7 M_{sun}
  - Halo finder yields location, mass, other properties of all galaxies, $M \geq 2.5 \times 10^9$ M_{sun}, "on-the-fly"

  e.g. $N_{halo} \sim 10^5$ by redshift $z \sim 11$

N-body + Radiative Transfer ➔ Reionization simulation

- Radiative transfer simulations evolve the radiation field and nonequilibrium ionization state of the gas

  - New, fast, efficient C^2-Ray code (Conservative, Causal Ray-Tracing) (Mellema, Iliev, Alvarez, & Shapiro 2006, *New Astronomy*, 11, 374) uses short-characteristics to propagate radiation throughout the evolving gas density field provided by the N-body results, re-gridded to $(203)^3$ and $(406)^3$ cells, for different resolution runs, from each and every galaxy halo source in the box.

  e.g. $N_{halo} \sim 10^5$ by redshift $z \sim 11$

Structure formation in ΛCDM at z = 10

simulation volume = $(100\ h^{-1}\mathrm{Mpc})^3$, comoving

1624^3 particles on 3248^3 cells

Projection of cloud-in-cell densities of 20 Mpc slice

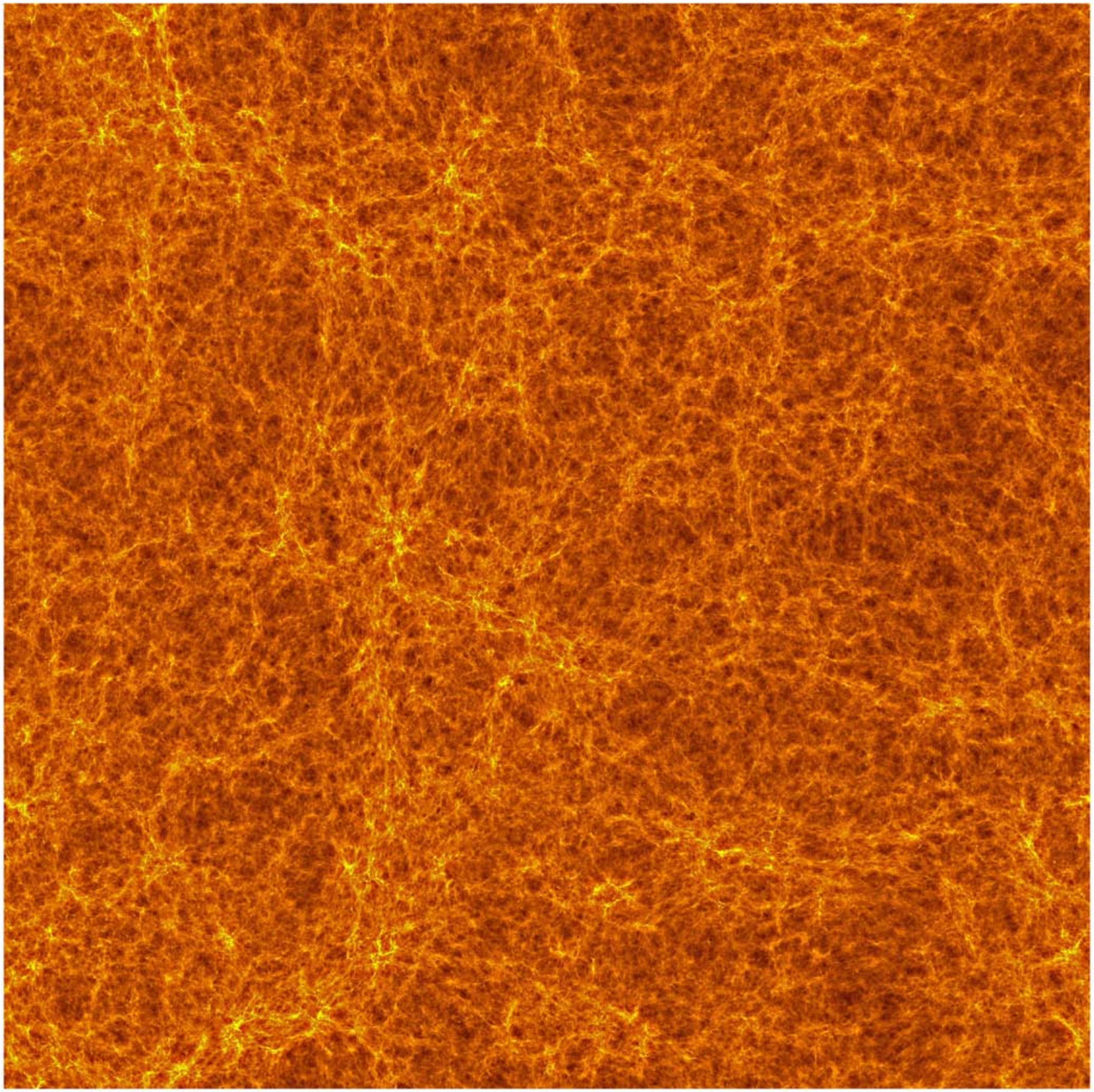

Every galaxy in the simulation volume emits ionizing radiation

- We assume a constant mass-to-light ratio for simplicity:

f_γ = # ionizing photons released by each galaxy per halo baryon

$= f_* \; f_{esc} \; N_i$,

where f_* = star-forming fraction of halo baryons,

f_{esc} = ionizing photon escape fraction,

N_i = # ionizing photons emitted per stellar baryon over stellar lifetime

e.g. $N_i = 50{,}000$ (top-heavy IMF), $f_* = 0.2$, $f_{esc} = 0.2$ ➔ $f_\gamma = 2000$

Every galaxy in the simulation volume emits ionizing radiation

- We assume a constant mass-to-light ratio for simplicity:

f_γ = # ionizing photons released by each galaxy per halo baryon

$= f_* \; f_{esc} \; N_i$,

where f_* = star-forming fraction of halo baryons,

f_{esc} = ionizing photon escape fraction,

N_i = # ionizing photons emitted per stellar baryon over stellar lifetime

e.g. $N_i = 50{,}000$ (top-heavy IMF), $f_* = 0.2$, $f_{esc} = 0.2$ ➔

$f_\gamma = 2000$

- This yields a source luminosity: $dN_\gamma/dt = f_\gamma \; M_{bary} / t_*$,

t_* = source lifetime (e.g. 2×10^7 yrs),

M_{bary} = halo baryonic mass

Evolution of the Mean Ionized Fraction of the Universe

- First sources start forming at z = 21

- H II regions finally overlap to finish reionization at z = 11.3

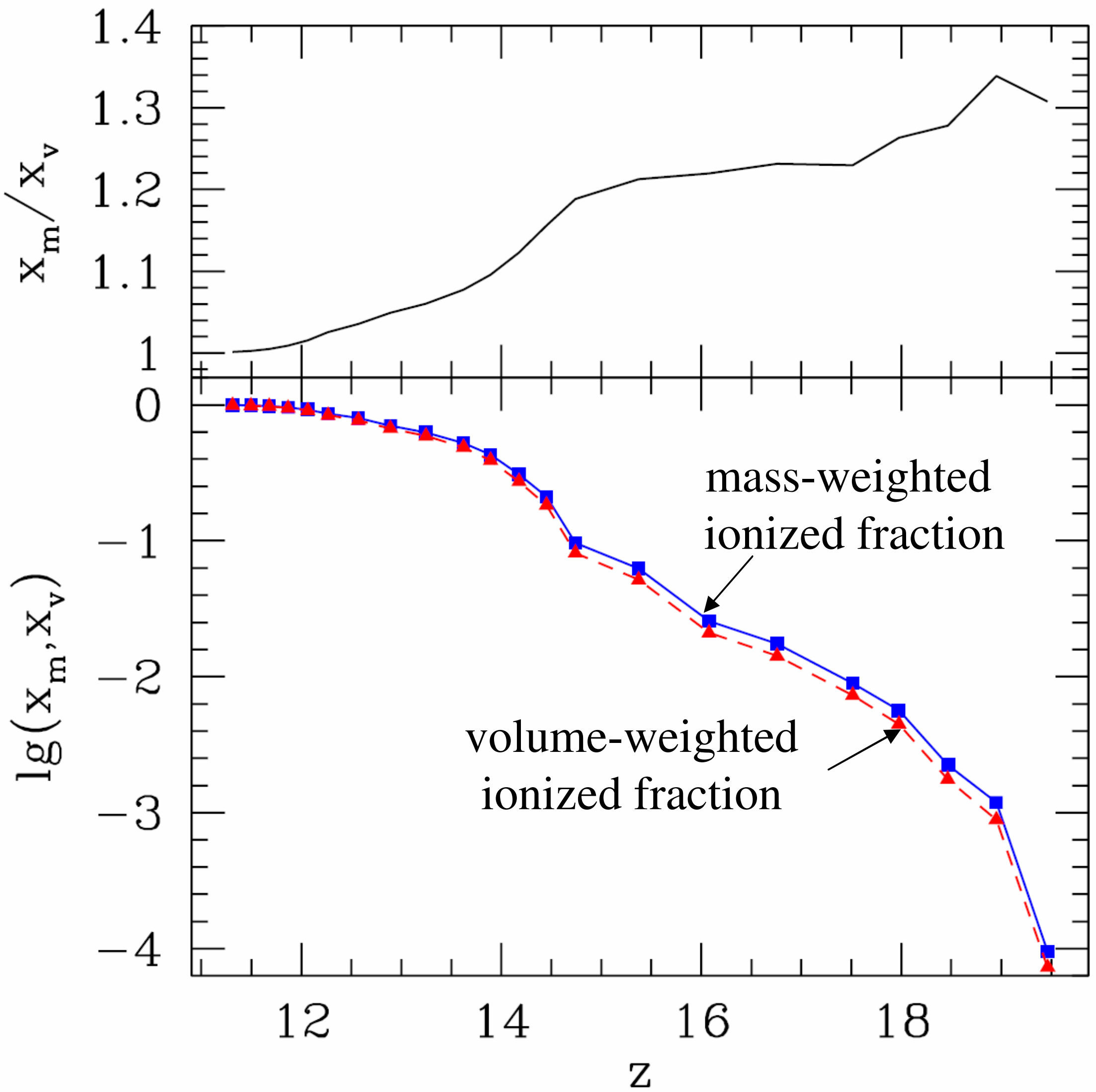

x_m = mass-weighted

x_v = volume-weighted

(f_γ = 2000)

Time-slices of the reionization simulation ($f_\gamma = 2000$)

z = 18.5 16.1 14.5

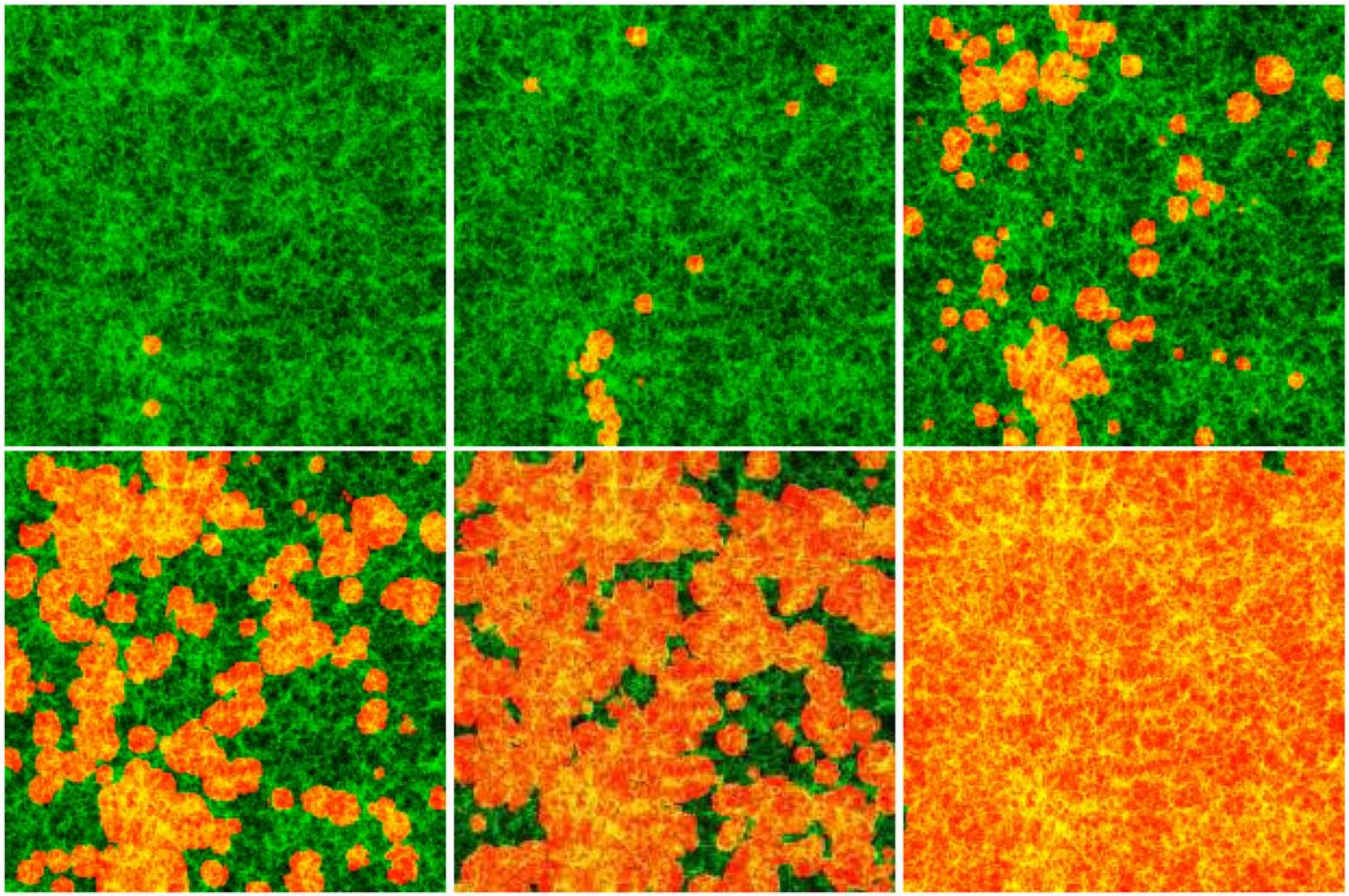

13.6 12.6 11.3

Reionization proceeds “inside-out” from high-density to low-density regions

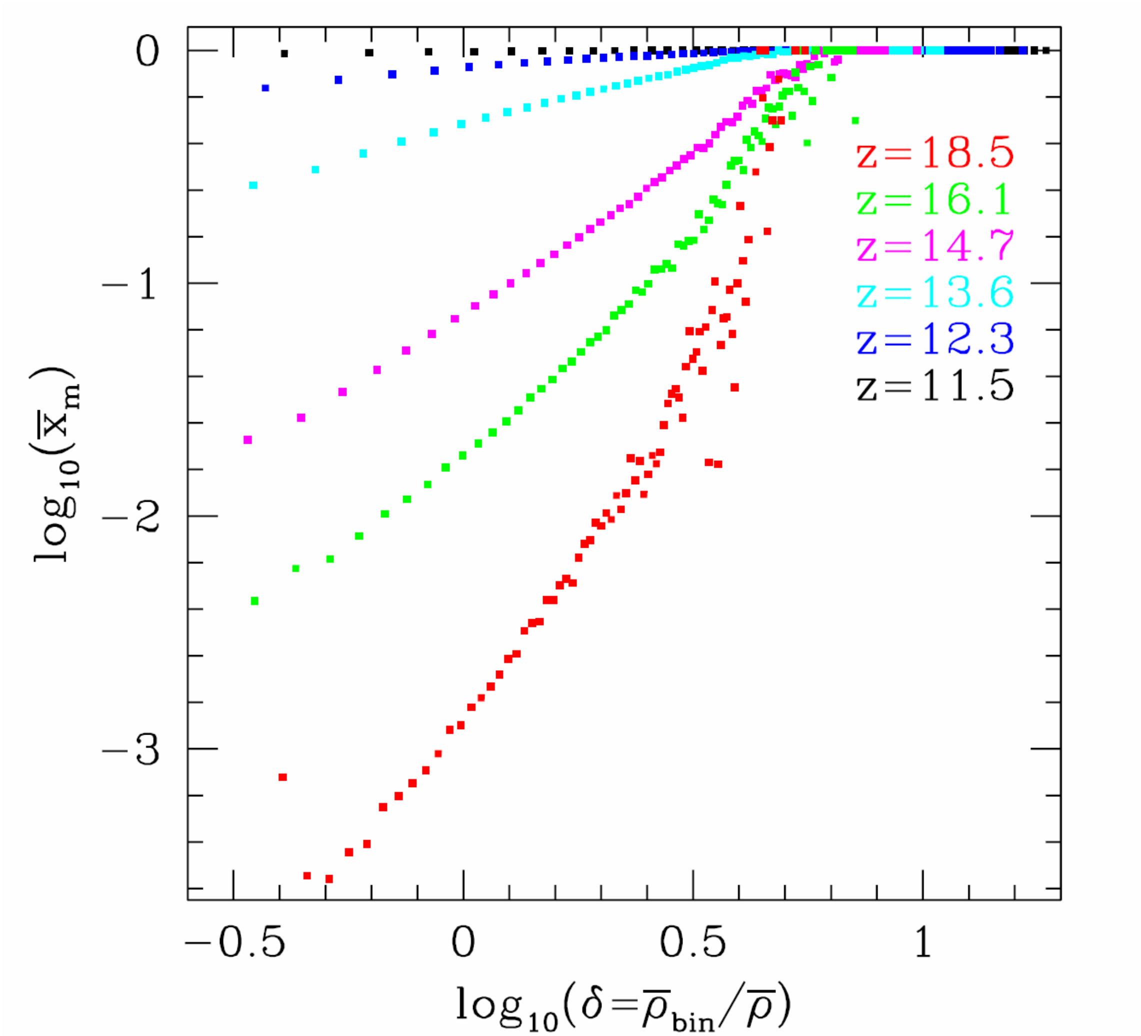

A 3-D view of the H II regions in the simulation volume as the mean ionized fraction of the universe approaches 50% (f_γ = 2000)

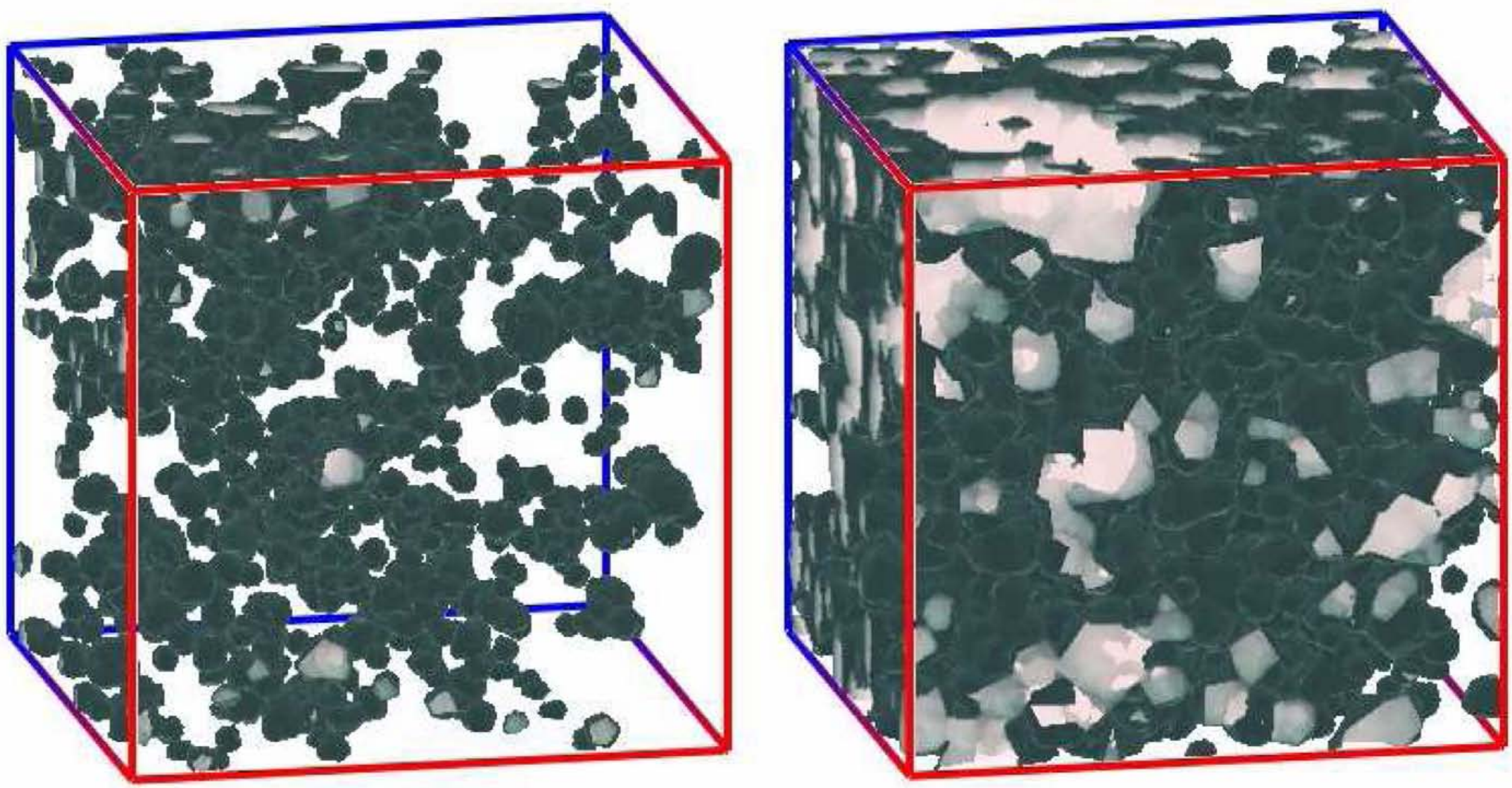

z = 14.74 z = 13.62

The Geometry of Reionization

for source efficiency
$f_\gamma = 2000$

from z = 19.5 to z = 13.2

a cut through the simulation volume, one cell deep

gas density (green in neutral regions, yellow in ionized regions)
and
the H II regions (red)

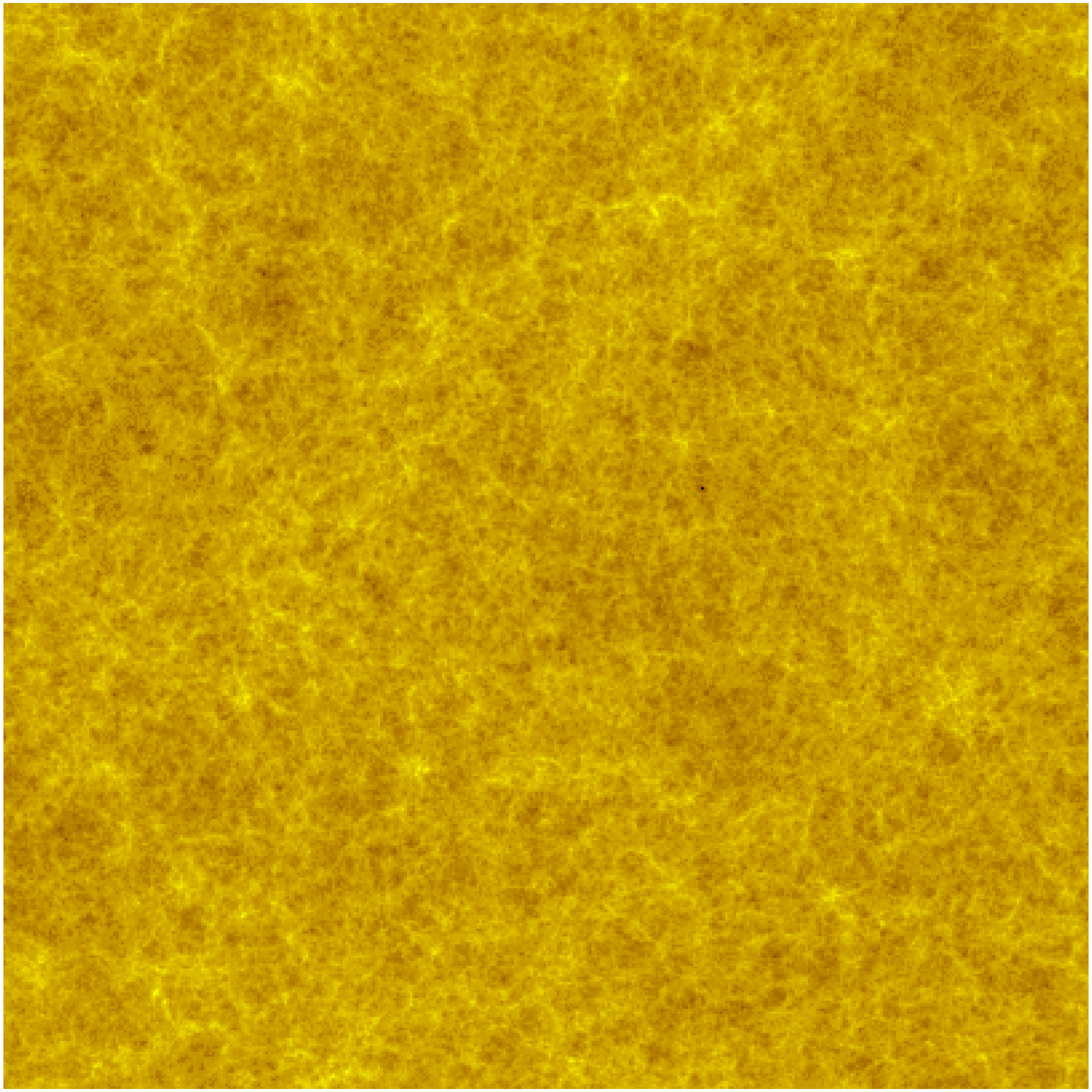

Subregions reionize at different times.

• The mean ionized fractions in independent subregions of the simulation volume differ considerably from the global mean.

• There is a large scatter in the value of z_{ov} about the global average.

• The larger the subregion, the smaller is the scatter, but need $V > 30\ h^{-1}$ Mpc to make $\Delta z < 2$.

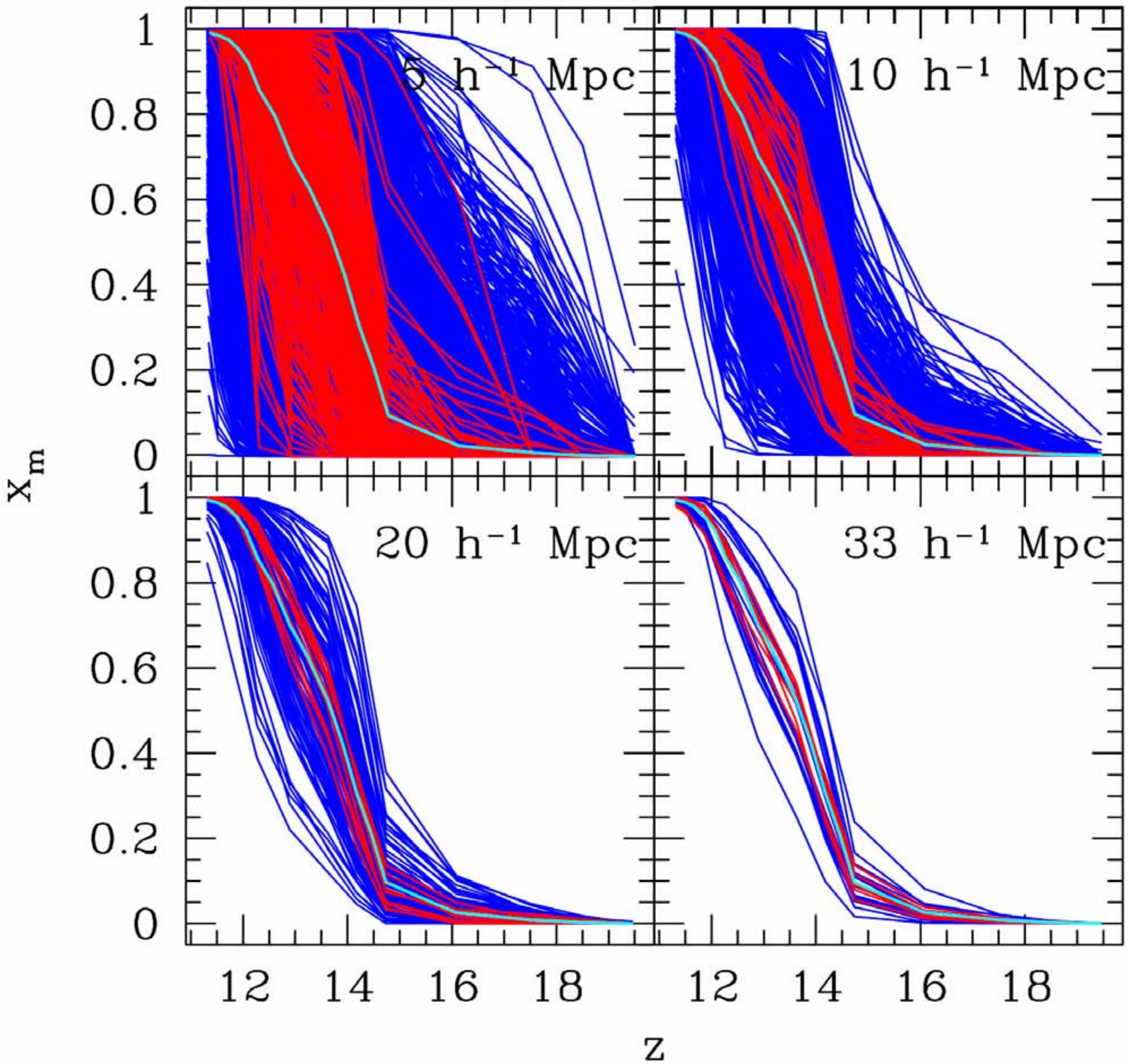

Self-Regulated Reionization

Iliev, Mellema, Shapiro, & Pen (2006), MNRAS, submitted;

(astro-ph/0607517)

Extended reionization: Jeans-mass filtering, halo-mass-dependent emissivity

<u>Cases</u>

1. Halo masses $M_{solar} > 10^9$
   $f_\gamma = 2000$ (e.g. Pop III);

2. Halo masses $M_{solar} > 10^9$
   $f_\gamma = 250$ (e.g. Pop II);

3. Halo masses $M_{solar} > 10^8$
   $f_\gamma = 250$ (e.g. Pop II),
   lower-mass halos
   suppressed inside H II regions
   (Jeans-mass filtering) ;

4. Same as 3., but
   $f_\gamma = 2000$ ($M_{solar} < 10^9$)
   $f_\gamma = 250$ ($M_{solar} > 10^9$)

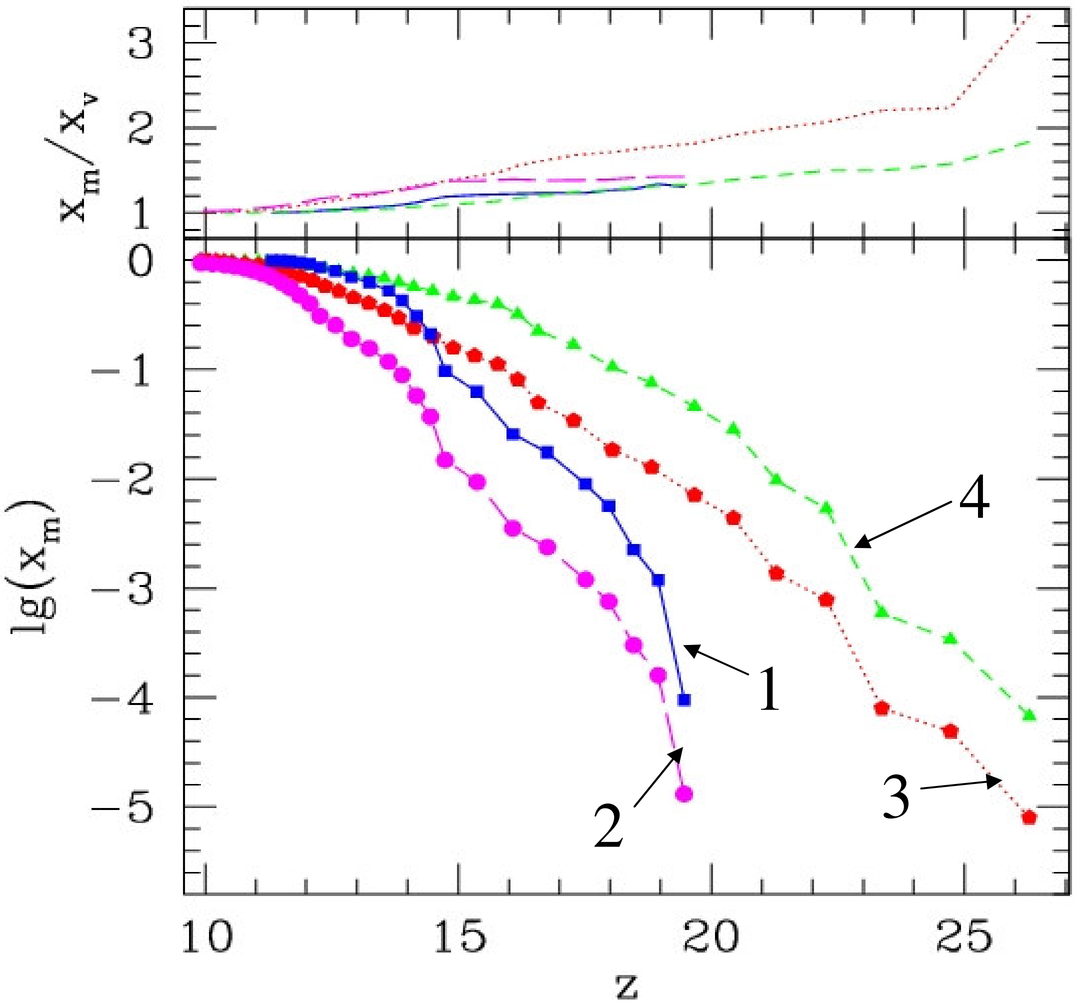

Extended reionization: Jeans-mass filtering, halo-mass-dependent emissivity

Cases

1. Halo masses $M_{solar} > 10^9$
   $f_\gamma = 2000$ (e.g. Pop III);

2. Halo masses $M_{solar} > 10^9$
   $f_\gamma = 250$ (e.g. Pop II);

3. Halo masses $M_{solar} > 10^8$
   $f_\gamma = 250$ (e.g. Pop II),
   lower-mass halos
   suppressed inside H II regions
   (Jeans-mass filtering) ;

4. Same as 3., but
   $f_\gamma = 2000$ ($M_{solar} < 10^9$)
   $f_\gamma = 250$ ($M_{solar} > 10^9$)

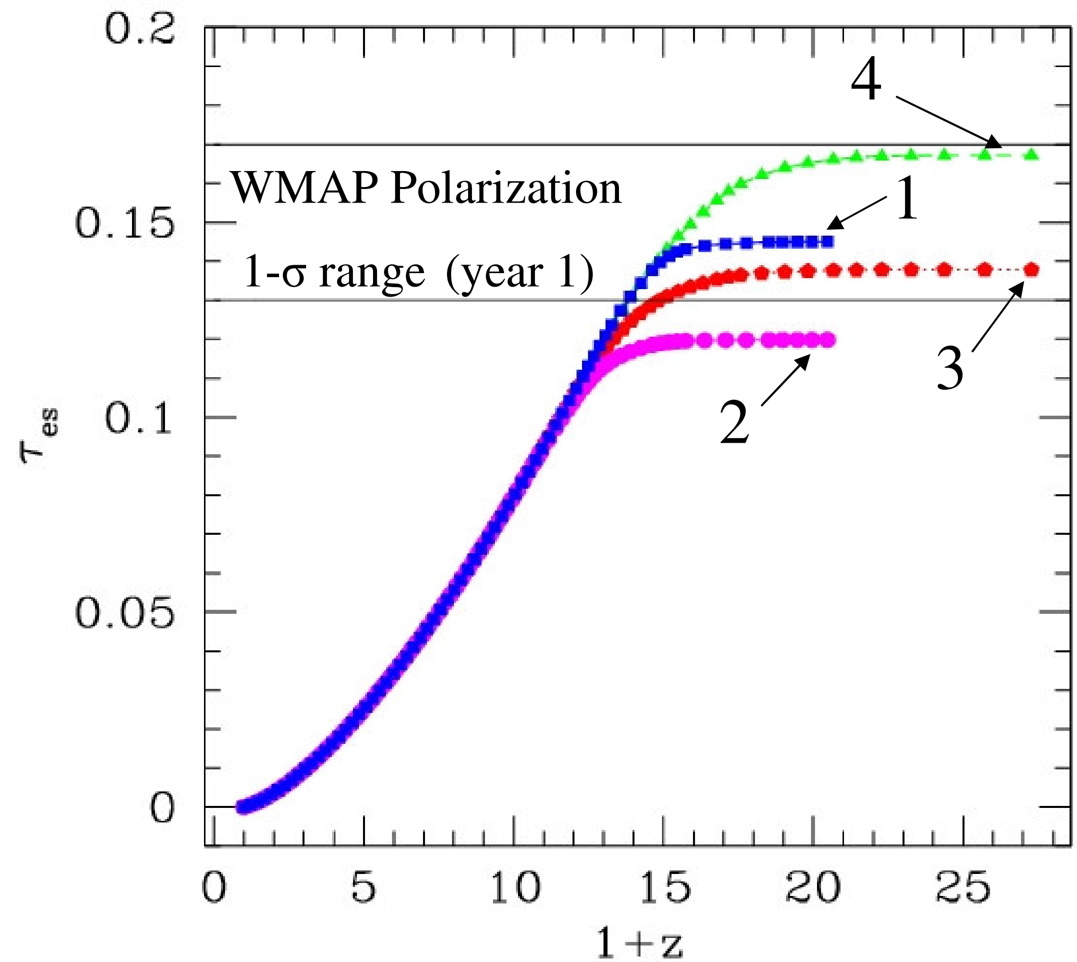

Simulating Cosmic Reionization at Large Scales II : The 21-cm Emission Features and Statistical Signals

Mellema, Iliev, Pen, & Shapiro (2006) MNRAS, in press
astro-ph/0603518

Q: How large must a reionization simulation volume be to predict 21-cm background fluctuations?

- Simulation volumes must exceed the beamsize and bandwidth of future radio arrays by a large enough factor to make 21-cm predictions meaningful.

e.g. for PAST, LOFAR,

$\Delta\theta_{beam} \geq 3'$

$\Delta\nu_{bandwidth} > 0.1$ Mhz

- Our (143 Mpc)^3 comoving volume simulation is the first to be large enough to predict 21-cm fluctuations.

$L_{box} = 100\ h^{-1}$ Mpc (comoving)

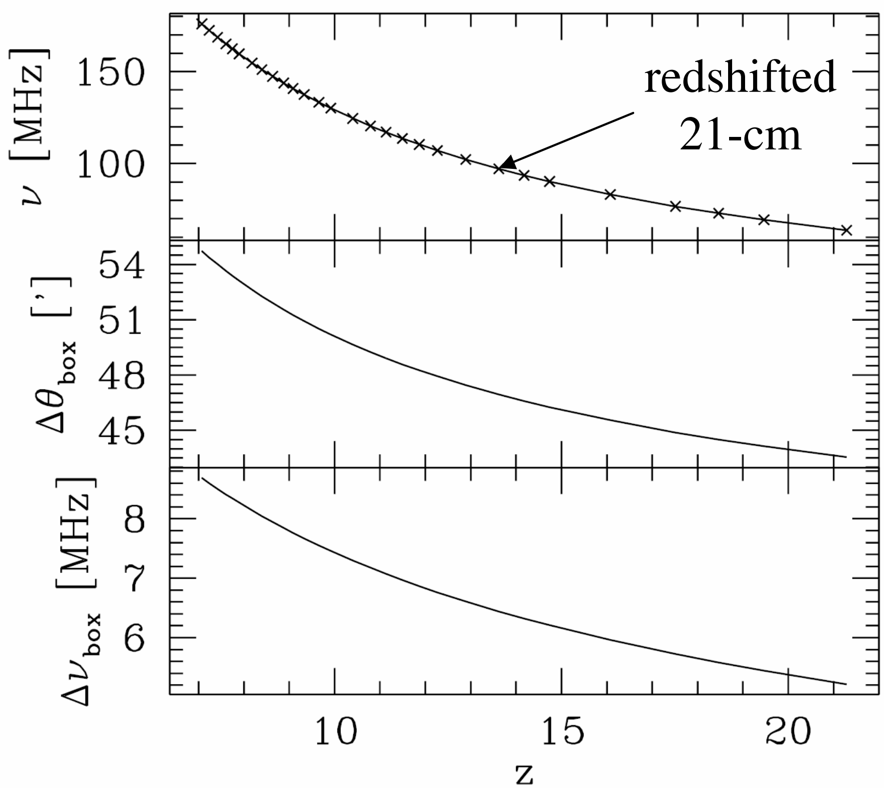

Evolution of the Mean 21-cm Brightness Temperature

	f2000	f2000_406	f250	f2000C
mesh	203^3	406^3	203^3	203^3
f_γ	2000	2000	250	2000
$C_{\rm subgrid}$	1	1	1	$C(z)$
$z_{50\%}$	13.6	13.5	11.7	12.6
$z_{\rm overlap}$	11.3	~ 11	9.3	10.15
$\tau_{\rm es}$	0.145	~ 0.14	0.121	0.135

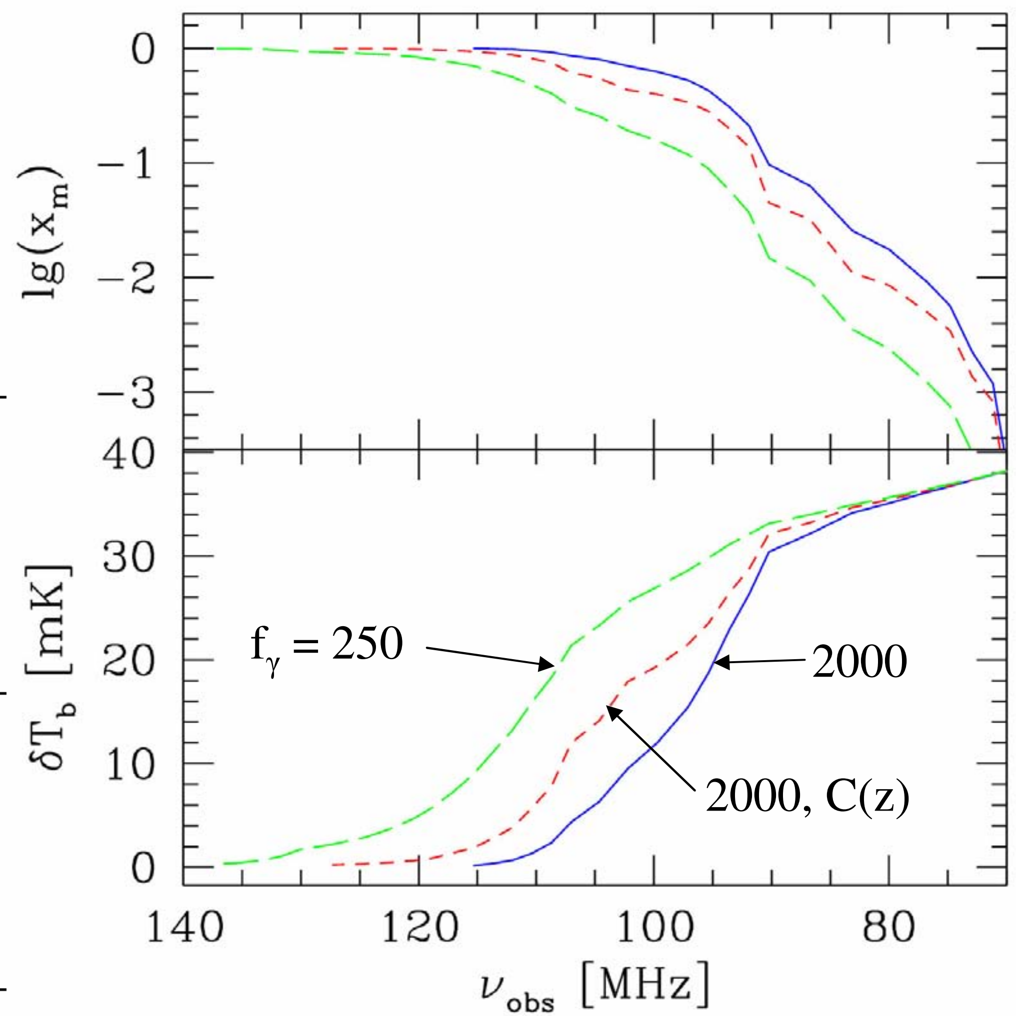

- Suggestion that a "global reionization step" in frequency space would make mean 21-cm emission signal detectable (Shaver et al. 1999) appears more difficult than previously thought <===> reionization more gradual on average
- Lower efficiency f_γ *delays*, while subgrid clumping C(z) *extends* reionization.

Reionization topology revealed by fluctuations in 21-cm brightness temperature, δT_b , along the line of sight

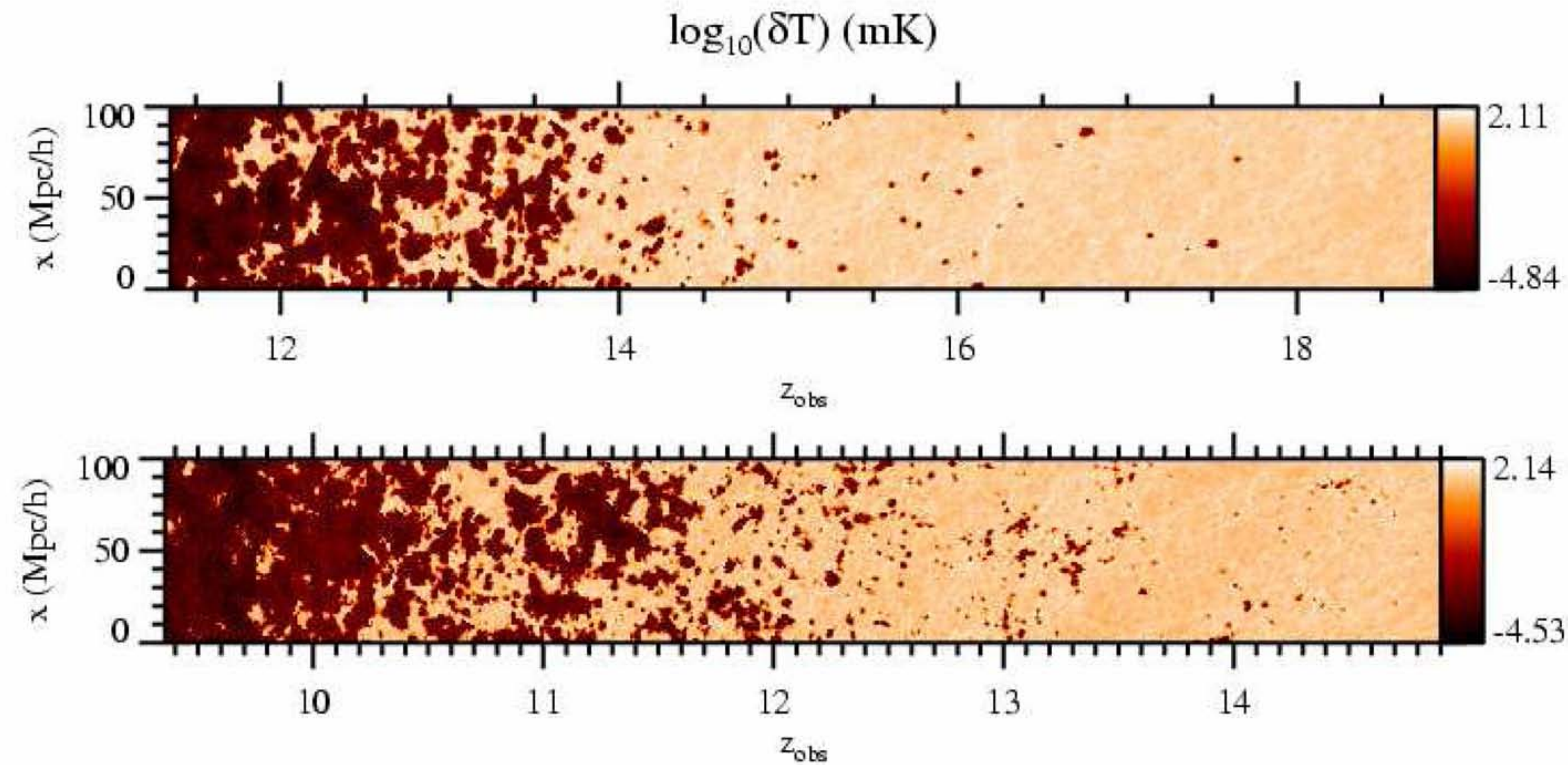

- Mapping the sky along the line of sight : cuts in position-redshift space for two different simulations:

Cases f2000 (top) and f250 (bottom)

21-cm sky maps

Case f 2000

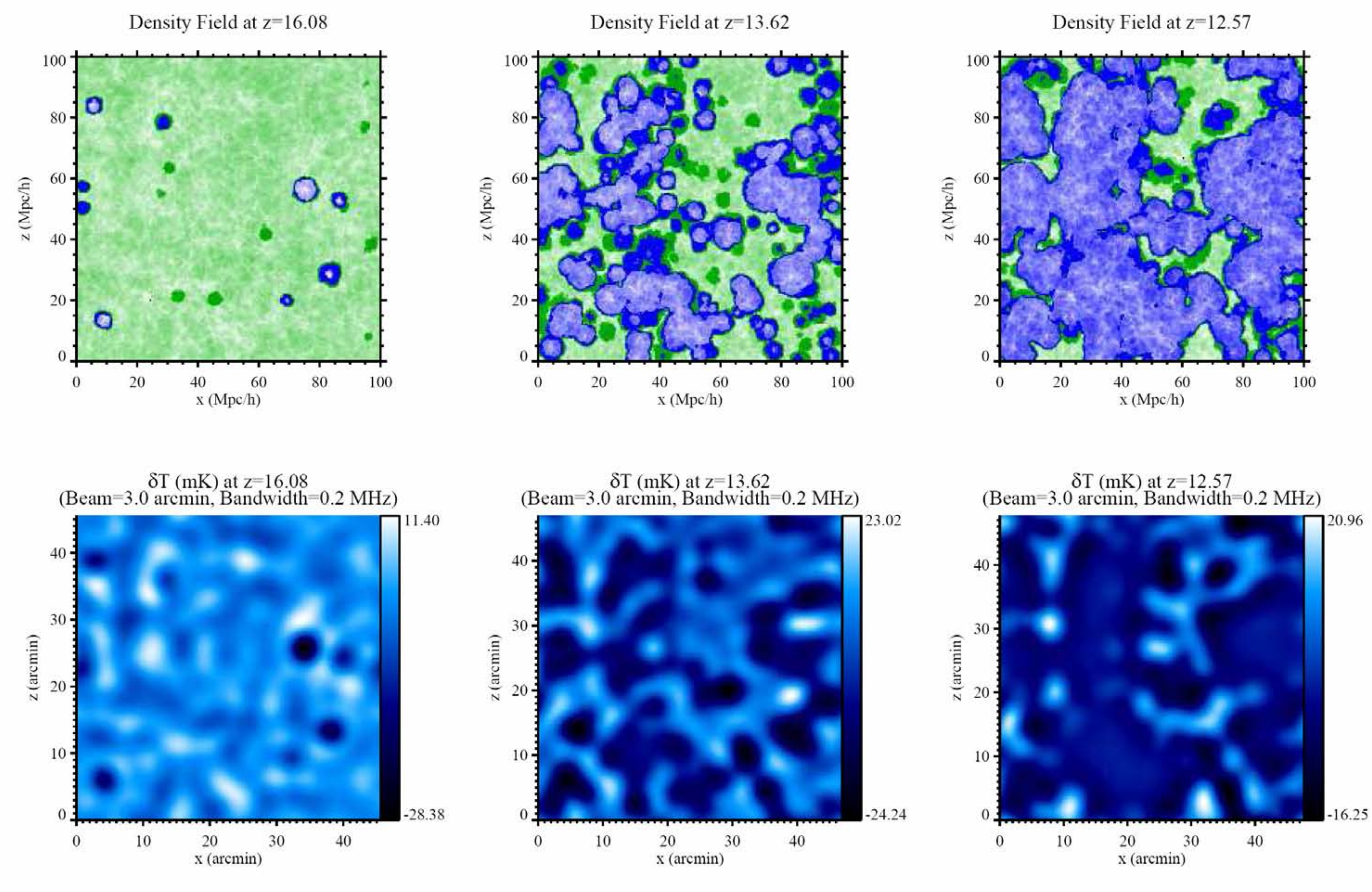

Subtracted 21-cm sky maps

- To eliminate foreground contamination, we subtract the band-averaged signal in a wide frequency band (e.g.$\Delta\nu$ =5MHz)

  from the signal within the observed bandwidth

(e.g. $\Delta\nu$ = 0.2MHz)

- Signal survives subtraction.

Case f 250

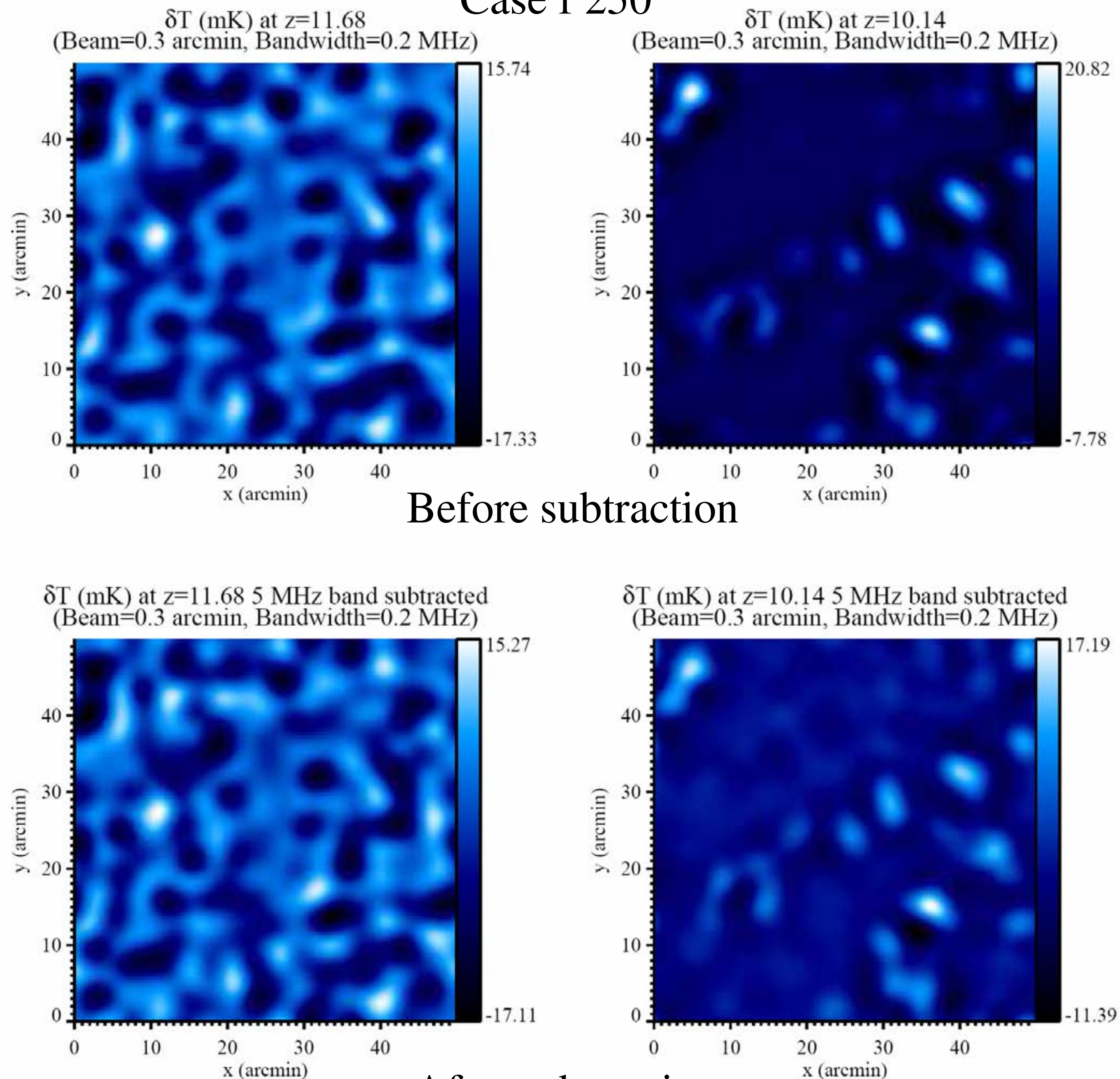

Before subtraction

After subtraction

21-cm sky maps : rare, bright peaks

- Brightest emission peaks may be easiest features to detect.
- Peak values decline more slowly with time than mean signal.
- Figure key

(#, #) =

($\Delta\theta_{\text{beam, arcmin}}$, $\Delta\nu_{\text{bandwidth,MHz}}$)

(6, 0.4) <===> e.g. PAST

(3, 0.2) <===> e.g. LOFAR

(1, 0.1) <===> e.g. SKA

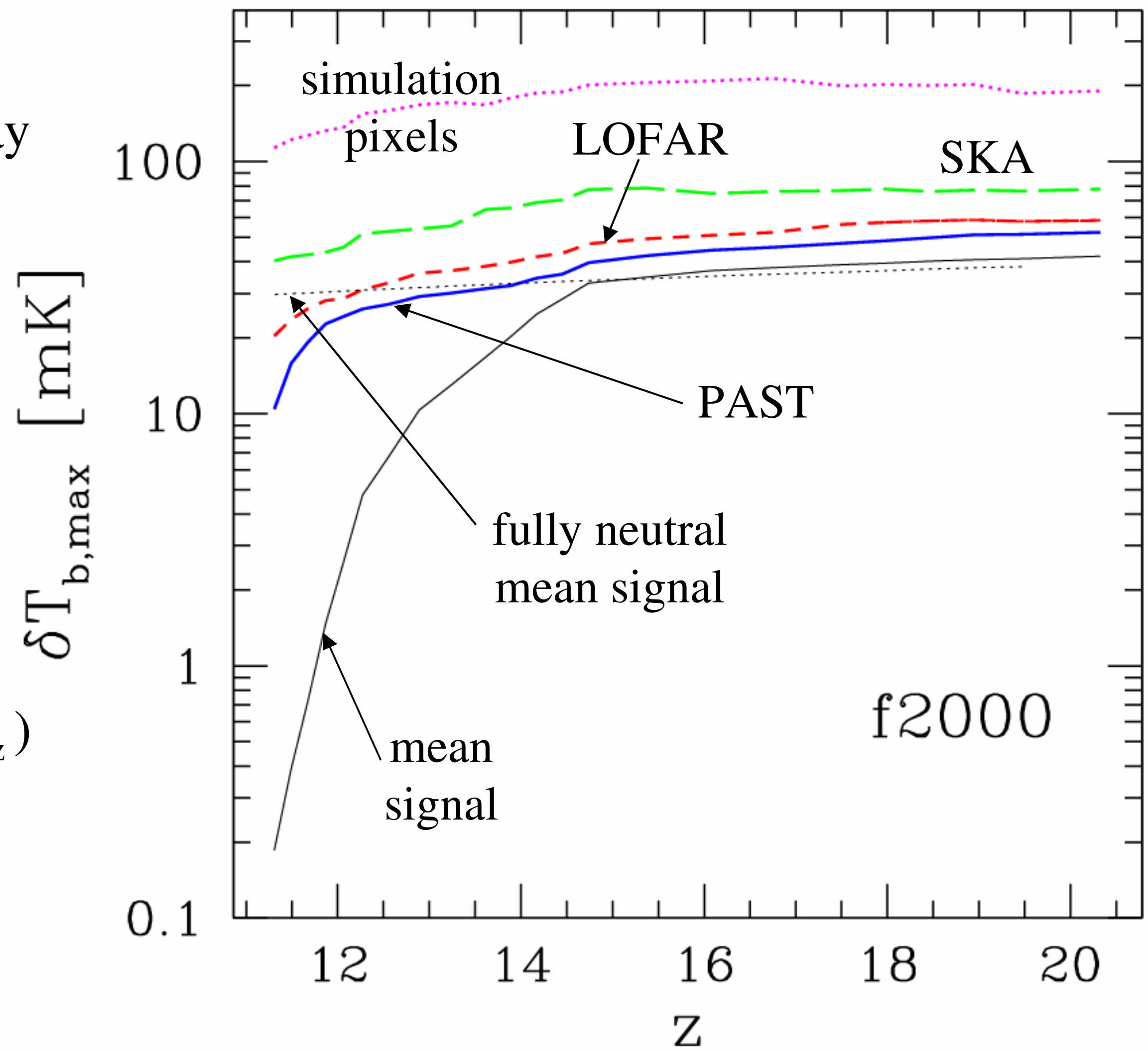

21-cm line-of-sight spectra

$f_{\gamma} = 250$

- **Spectra at full simulation resolution** (red):
  $(\Delta\theta\ ,\ \Delta\nu)_{cell} \sim$ (14", 30 kHz) for $(203)^3$ cells.

- **Smoothed spectra** (blue):
  $\Delta\nu_{bandwidth,MHz} = 0.2 MHz$
  $\Delta\theta_{beam,\ arcmin} = 3$ arcmin

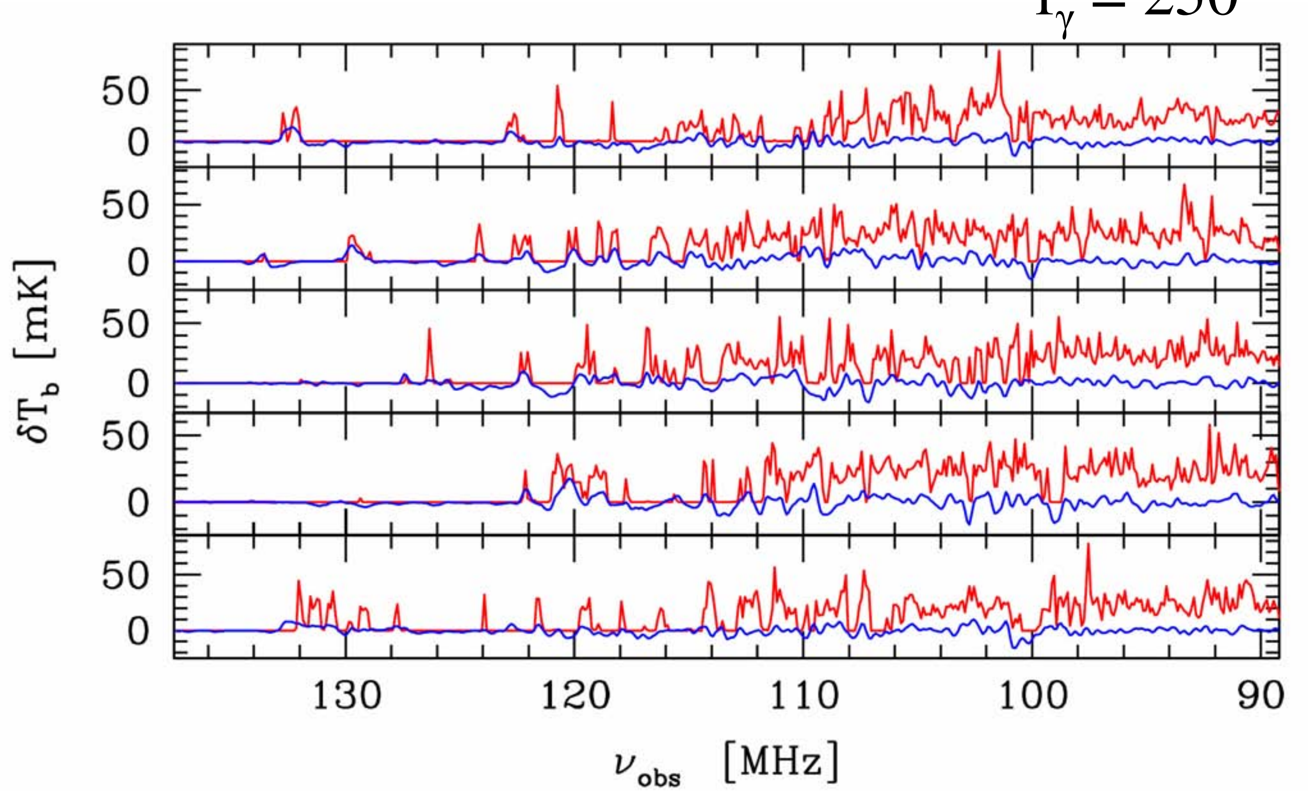

- Smoothing beam is a compensated Gaussian (closer to radio observations than Gaussian), which produces negative δT_b at the minima.
- At high z (ν < 100 MHz), when IGM mostly neutral, smoothing reduces signal, due primarily to density fluctuations.
- Once H II regions multiply and grow (ν >100 MHz), fluctuations increase, creating valleys deeper than the neutral density peaks ➔ easier to detect?

21-cm 2-D angular power spectra

- Power spectrum peaks at $\ell = \ell_{max}$, with ℓ_{max} ↓ as z ↓ then leveling off.

e.g. For f 2000, unsmoothed, max ~ 10 mK at ℓ_{max} ~ 4000 (~ 5') at z = 13.6, when <x> ~ 50% .

Case f 250 similar, except ℓ_{max} ~ 5000 (~ 4') at z = 11.8.

- Density fluctuations are smaller than those of brightness temperature.

f 2000

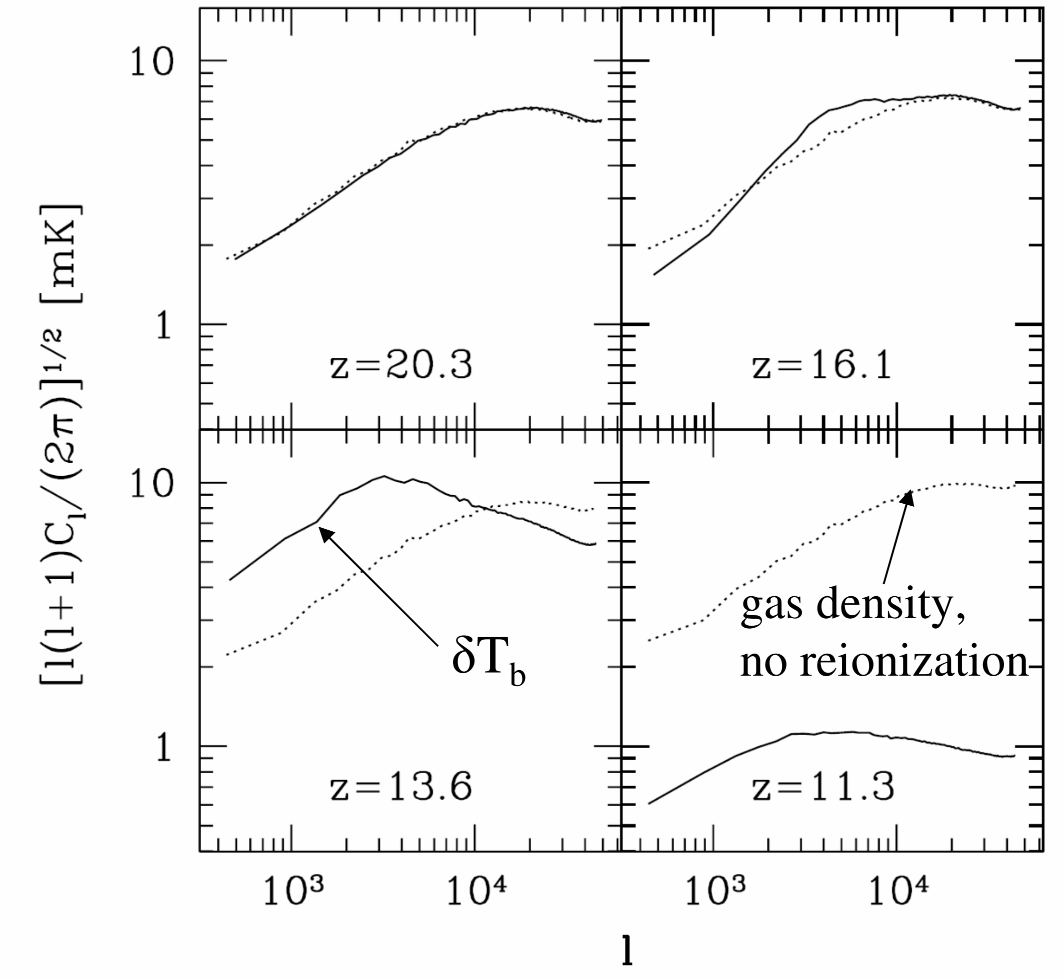

The Kinetic Sunyaev-Zel'dovich Effect from Radiative Transfer Simulations of Patchy Reionization

Iliev, Pen, Bond, Mellema, & Shapiro (2006), ApJ, submitted; and

(2006) New Astronomy Reviews, in press

(astro-ph/0607209)

Kinetic Sunyaev-Zel'dovich from Patchy Reionization

- kSZ effect is the CMB temperature anisotropy induced by electron scattering by free electrons moving along the line-of-sight:

$$\frac{\Delta T}{T_{\rm CMB}} = \int d\eta e^{-\tau_{\rm es}(\eta)} a n_e \sigma_T \mathbf{n} \cdot \mathbf{v},$$

where η is conformal time,

$$\eta = \int_0^t dt'/a(t')$$

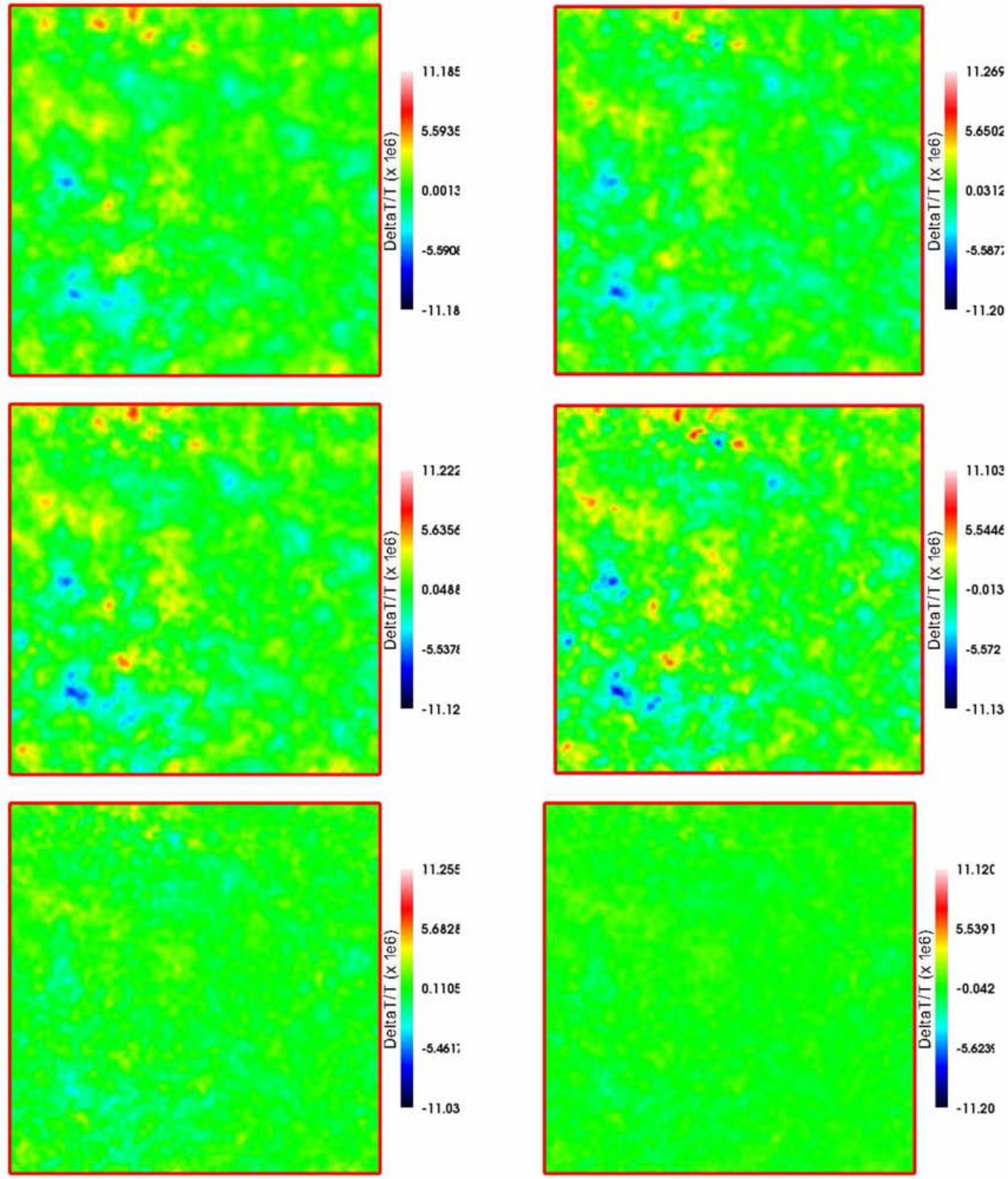

FIG. 1.— kSZ maps from simulations: f2000 (top left), f250 (top right), f2000C (middle left), f250C (middle right) instant reionization at $z_{\rm instant}$ = 13 which gives the same total electron scattering optical depth as simulation f250 (bottom left), and spatially-uniform reionization with the same reionization history and thus same total electron scattering optical depth as simulation f250 (bottom right). (Images produced using the Ifrit visualization package of N. Gnedin).

kSZ CMB Anisotropy Signal:
$\delta T_{kSZ} / T_{CMB}$ 2-D angular power spectra

- kSZ anisotropy from inhomogeneous reionization dominates primary CMB anisotropy for $\ell > 3000$, peaking at $\ell = \ell_{max} = 2000 – 8000$, determined by typical sizes of H II regions, 5 – 20 Mpc.

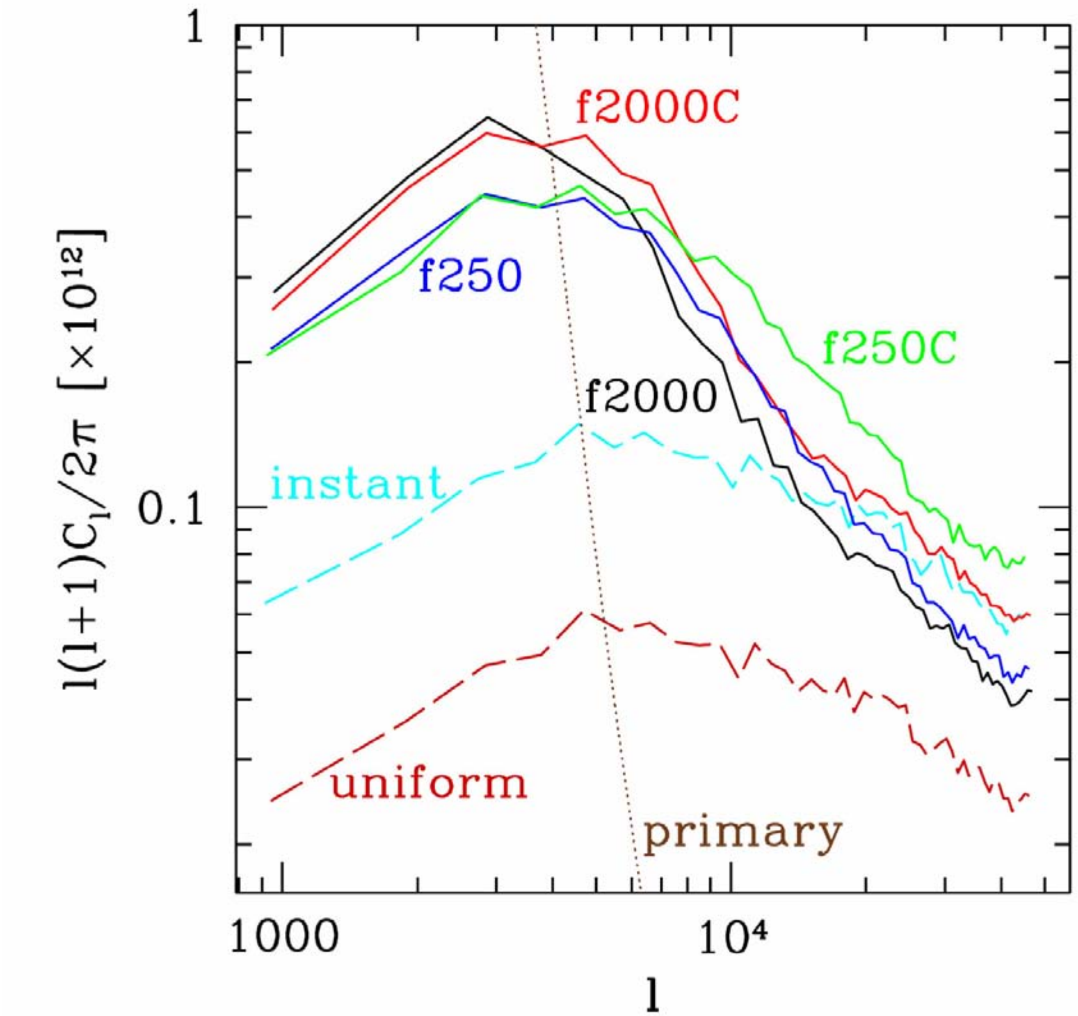

- Patchy reionization doubles total kSZ for $\ell = 3000 – 10{,}000$, compared to instant reionization approximation.

- This predicted kSZ signal at arcminute scales should be detectable by upcoming experiments. e.g. Atacama Cosmology Telescope, South Pole Telescope, (~ 1' resolution, ~ μK sensitivity)